Novel discrimination of biuret and triuret degradation by enzymatic deamination, Regulation and significance for slow-release nitrogen fertilizers

---

A THESIS

SUBMITTED TO THE FACULTY OF THE GRADUATE SCHOOL

OF THE UNIVERSITY OF MINNESOTA

BY

Lambros J. Tassoulas

IN PARTIAL FULFILLMENT OF THE REQUIREMENTS

FOR THE DEGREE OF

MASTER OF SCIENCE IN MICROBIAL ENGINEERING

Professor Lawrence P. Wackett, Advisor

August, 2019

Acknowledgments

Firstly, I would like to express my gratitude to my advisor, Prof. Larry Wackett, for giving me the opportunity to work in his research group on a project that I am very motivated to pursue and constantly gives me more to think about. I have gained knowledge and experience in multiple areas of science as a result and I am very grateful for this and the contributions I have made so far. Dr. Wackett's vast knowledge, guidance have helped shape both this thesis and myself as an aspiring researcher.

I would like to thank Dr. Mikael Elias for his advice and company during the crystallography experiments. I really appreciate that I went through this endeavor and when I had disbelief of crystallizing the protein, Dr. Elias was there to encourage me to keep trying.

Special thanks goes to Jack Richman, Tony Dodge, Serina Robinson, Kelly Aukema, Céline Bergonzi, Sudipta Shaw and to the rest of my colleagues in the Gortner laboratory who are a joy to work with and for the fruitful discussions we have had, as well as their company.

I would like to dedicate this thesis to my father, Yannis Tassoulas, for being a big influence in my life which I am grateful for.

Lambros Tassoulas , Minneapolis, July 4, 2019

The work in this Thesis was supported by grants from the University of Minnesota Grand Challenges Initiative and BTI-MnDRIVE.

Abstract

Triuret (carbonyl diurea) is an impurity of industrial urea fertilizer (<0.2%) which results in several hundred thousand tons applied, worldwide, each year on agricultural lands. Triuret has been described in the literature as early as 1870 when it was first synthesized and, although the natural source of triuret is unknown, it is hypothesized to be from oxidative uric acid metabolism. The biodegradation of triuret was known but, prior to this work, no enzymes had been identified. The triuret decomposing enzyme (TrtA) was discovered by observing two paralogs in gene clusters, one of which was well characterized as a biuret hydrolase (BiuH). TrtA, an amidohydrolase from the isochorismatase hydrolase like superfamily (IHL), similarly to BiuH, has a catalytic efficiency (k_{cat}/K_M) of 6×10^5 ($M^{-1}s^{-1}$) and a K_M for triuret in the μM range with narrow substrate specificity. Crystal structures of TrtA in apo and holo form were solved which show an intriguing comparison with the BiuH structure where second shell residues around the near-identical active sites direct the specificity for each native substrate. With this discovery, the regulation of the triuret degradation operon, which can direct the mineralization of triuret completely to ammonium and carbon dioxide, was investigated in *Herbaspirillum* sp. BH-1. The operon was shown to be specifically induced by biuret or triuret and suppressed in nitrogen sufficient conditions. Interestingly, the triuret hydrolase genes in the RefSeq database (<1%) come largely from plant-associated bacteria that can nodulate or are known endophytes and the broader context of this metabolism remains to be seen. As metabolism of triuret is relatively rare, and triuret is far less soluble in water than urea or ammonium nitrate, triuret may be considered a potential slow release N fertilizer.

Contents

Acknowledgments i

Abstract ii

List of Figures v

List of Tables vii

1 Introduction 1

1.1 Motivation 5

1.2 Thesis contributions 5

1.3 Thesis outline 6

1.4 Notational conventions 6

2 Discovery and structural analysis of a triuret hydrolase from the biuret degradation pathway in *Herbaspirillum sp. BH-1* **7**

2.1 Introduction 7

2.2 Methods 11

2.3 Results 13

2.4 Discussion 26

3 Regulation of the triuret degradation pathway in *Herbaspirillum* sp. BH-1: Discovery of carboxybiuret decarboxylation function from two structurally divergent enzymes **31**

3.1 Introduction 31
3.2 Methods 36
3.3 Results 39
3.4 Discussion 47

4 Application and Future Research 53

4.1 Triuret: A potential N fertilizer 53
4.2 Industrial synthesis 54
4.3 Fertilizer Demonstration 55
4.4 Conclusion and Future Research 55

Bibliography 58

A Supplementary Information 64

List of Figures

1.1 Side Reactions in Industrial Urea Synthesis 3
1.2 Nitrogen Fertilizer: The Grand Challenge 5

2.1 Triuret and Cyanuric Acid Mineralization Pathways through Biuret 8
2.2 Multiple Sequence Alignment of TrtA with related IHL Superfamily Members 10
2.3 Elucidation of the Reaction Product of TrtA by ^{13}C NMR 16
2.4 Topology of TrtA 17
2.5 TrtA Dimer Structure 17
2.6 TrtA Active Site with Triuret 19
2.7 Comparison of Triuret structure in TrtA with Pure Triuret 20
2.8 Open-Closed Conformations of TrtA 21
2.9 Active site tunnel of TrtA 21
2.10 TrtA, BiuH Overall structure comparison 22
2.11 Active site comparison of TrtA and BiuH 23
2.12 TrtA Active Site with Biuret 24
2.13 Active Site mutagenesis of TrtA 25
2.14 Relative Triuret activity of TrtA variants against WT 26
2.15 Proposed Catalytic Mechanism for TrtA 28
2.16 Second-Shell residues around the Critical Gln Residue in TrtA and BiuH . . 30

3.1 Mineralization of Triuret through Biuret and Carboxybiuret 32
3.2 Gene Context of TrtA in *Herbaspirillum* sp. BH-1 33

3.3 Phylogenetic Tree and Taxonomy of Triuret Hydrolase 35
3.4 Induction of Triuret Hydrolase in *Herbaspirillum* sp. BH-1 grown on Various Nitrogen sources 40
3.5 Suppression of Triuret Hydrolase in *Herbaspirillum* sp. BH-1 in Starvation and Ammonium Rich Conditions 41
3.6 Gene contexts around TrtA revealing TrtB and Cupin genes 42
3.7 Multiple Sequence Alignment of TrtB with AtzH 43
3.8 Rate Enhancement of Triuret/Cyanuric Acid Mineralisation via TrtB 44
3.9 Multiple Sequence Alignment of Cupin Decarboxylases with related PDB structure 45
3.10 Activity of Cupin analogous to TrtB that is Metal Dependent 47
3.11 Gene Cooccurence with TrtA 49
3.12 Putative function of the gene *hpxZ* in the Allantoate metabolism pathway . 50

4.1 Proposed Industrial synthesis for Triuret 54

A.1 Thermal Stability of TrtA 64
A.2 TrtA Active Site with BME Adduct on Catalytic Cysteine 65

List of Tables

1.1 Properties of Urea Oligomers 2

2.1 Enzyme Kinetics of TrtA 14
2.2 Substrate Specificity of TrtA 15
2.3 Summary of X-ray Data Collection and Refinement 18

Chapter 1

Introduction

Nitrogen fertilizers have been in the spotlight in recent times as their leaching from agricultural lands is causing eutrophication of rivers, lakes and oceans which affects the native ecosystems established in these areas. The practice of nitrogen fertilizer is ancient. However, starting in the early 20th century, industrial scale ammonia and urea was developed to supply farmers with an inexpensive nitrogen fertilizer [1]. This in turn led to a significant increase in food production resulting in a population boom during this time. Industrially produced nitrogen fertilizers have been used ever since and the demand for them continues to increase every year while the environmental consequences of their use remain.

The amount of nitrogen that is taken up by crops from urea fertilizer has been estimated to be between 30%-50% where losses are attributed to the fast transformation of urea, by the soil microbiome, into ammonia and subsequent nitrification into nitrite and nitrate that leads to significant leaching [1]. A large proportion of microbes in the agricultural soils harbor the gene for urease and can hydrolyze urea to ammonia and CO_2 which consequentially leads to quick release of ammonia in a matter of a week. To counter this problem, urea has been modified in a few different ways including urea-formaldehyde resin, polymer coating of urea, or adding a urease inhibitor to slow the transformation. All of these modifications add significant cost and as a result these products are only used in residential application (gardens, golf courses, etc.) and are not feasible for agricultural use despite their ability to slow and fine-tune ammonia release into the soil.

Table 1.1: Properties of Urea Oligomers

Oligomer	m.p (°C)	Solubility (mM)	Applied 1000 tons/yr	Biuret Reaction
Urea	130	8000	80,850	None
Biuret	180	200	1238	Yes
Triuret	231	1.2	165	None
Tetrauret	200*	2	<12	Yes
Penturet	210*	0.1	<12	Yes

* thermal decomposition

The application of nitrogen fertilizer increases each year and food security depends on the crop yields that are achieved by using N inputs. Therefore, an economical, alternative nitrogen fertilizer must be developed to enact change, one that farmers can afford to buy and that guarantees similar crop yields. An alternative that has potential is triuret (carbonyldiurea), which is an oligomer of urea. Triuret is almost 8,000 times less soluble than urea and is actually a small impurity in urea fertilizer resulting in over 300 million pounds being applied worldwide each year (Table 1.1). Other impurities in urea are other oligomers including biuret, tetrauret and pentauret and these are formed by thermal decomposition of urea to form ammonia and reactive cyanic acid that can add onto biuret to form triuret and again to make tetrauret and so forth. The oligomerization of urea can hypothetically be indefinite as long as the oligomer is soluble or the reaction temperature is above its melting point although cyclization becomes very favorable for higher oligomers (triuret, tetra-, pentauret) to form cyanuric acid with ammonia, urea or biuret as the leaving group, respectively, so a mixture of products is usually found. The decreasing aqueous solubility trend with increasing oligomer size is most likely due to the planarity of the compounds with potential intramolecular hydrogen bonding, resulting in weak interactions with the solvent.

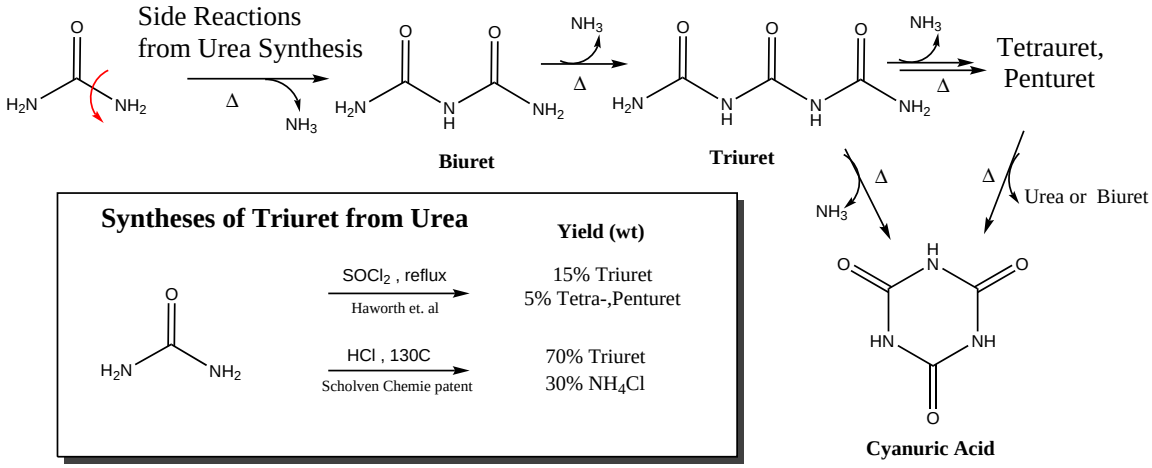

Figure 1.1: Side Reactions in Industrial Urea Synthesis
Urea can form oligomers by pyrolysis during industrial synthesis when urea splits into ammonia and reactive cyanic acid. Higher oligomers (triuret, tetra-, pentauret) also can cyclize into cyanuric acid to form a mixture products. The pyrolysis reactions can be acid-catalyzed by hydrogen chloride and thionyl chloride to form urea oligomers in higher yields. Scheme drawn in ChemDraw.

The oligomerization of urea can be acid-catalyzed to form triuret in higher yields with thionyl chloride and hydrogen chloride[2,3]. In both reactions the acids can help create ammonium salts which allow for more cyanic acid to be formed and cause urea oligomerization. The yield of the thioinyl chloride reaction is quite low for triuret as the sulfur can create side products and triuret is soluble in this solvent allowing for oligomerization into tetra- and pentaurets. The reaction of urea and HCl gas has a much better yield as when triuret is formed it is not soluble in the urea melt while biuret is, yielding mostly triuret and ammonium chloride.

The biodegradation of biuret has been well studied and that for triuret has now been discovered as described in Chapter 2[4,5]. As for the biodegradation of tetra- and pentauret, it is unknown and has not been studied but may follow a similar mechanism if it exists. Biuret was originally pursued as a potential N fertilizer but it has apparent toxic effects to crops (See Chapter 4). This may be caused by the chelation of divalent metal ions by biuret which is also observed for other urea oligomers except for triuret (Table 1.1). Triuret is unique of all of the urea oligomers for its high melting point and the crystal structure shows triuret in a *trans* conformation with intramolecular hydrogen bonding from the terminal

amines to the central carbonyl[6].

Triuret has been described in the literature as early as 1870 and is hypothesized to be a product of oxidative uric acid metabolism. Hydrogen peroxide and peroxynitrite can oxidize uric acid to generate triuret along with other products such as allantoin, which is a metabolite in the enzymatic degradation of uric acid[7]. While hydrogen peroxide can make triuret as a minor product of uric acid oxidation, peroxynitrite is far more selective and yields triuret as the major product in aqueous solution. Peroxynitrite is formed from nitric oxide and superoxide and can cause nitration of tyrosine residues in proteins[47]. Uric acid can then be considered a natural scavenger of oxidative species which may be a reason for the lack of urate degradation enzymes in humans for added fitness[8]. In smokers and women experiencing preeclampisa, who are undergoing oxidative stress, triuret can be detected in urine samples at significant levels. In freshwater amoebas, triuret granules are observed within the cell, suggesting that triuret is formed physiologically[9,10]. One study was able to isolate a *Corynebacterium* species that degrades triuret but the enzymes involved were unknown up until the point of the publication of this thesis[11].

1.1 Motivation

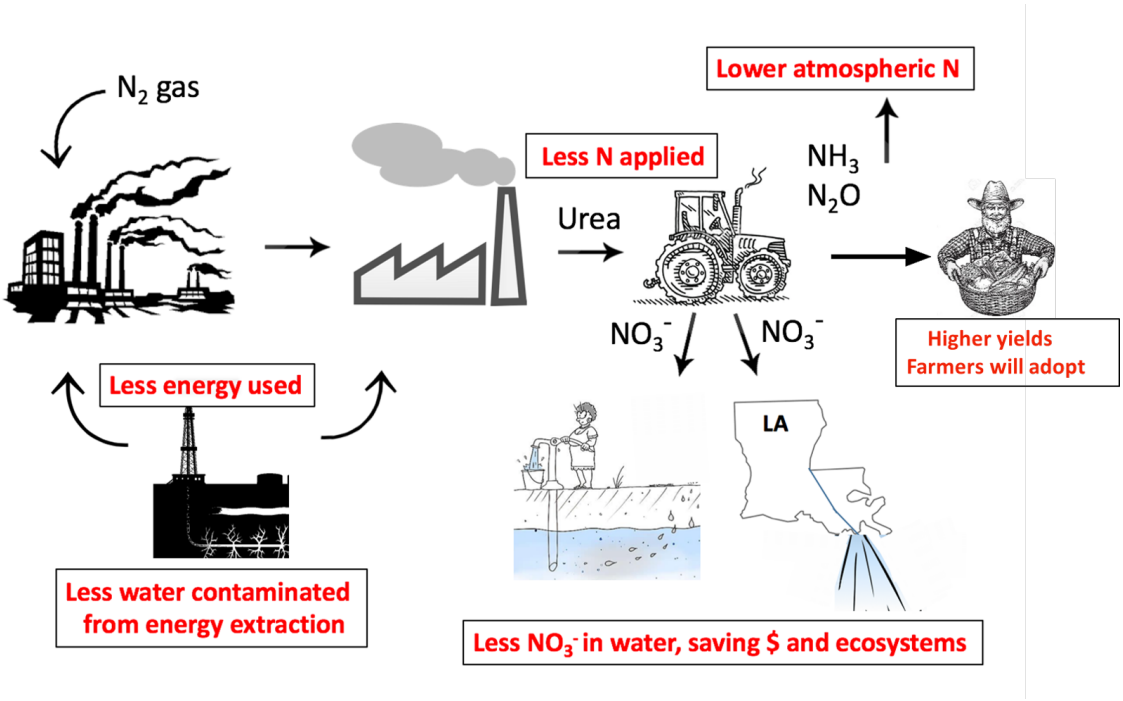

Figure 1.2: Nitrogen Fertilizer: The Grand Challenge

If the enzymes involved in triuret metabolism were known then the genes that encode them could then be identified in recorded genomes and help model triuret mineralization in soils in the context as a nitrogen fertilizer. The goal is to see the efficiency of nitrogen fertilizer utilization by plants increasing from ∼30%, currently with urea, to >60% with triuret. If triuret as a fertilizer becomes a reality then there are many benefits starting with less nitrogen needed to be applied to fields, which leads to less leaching of nitrogen away from farm lands. Waters will be less polluted, saving money on water treatment and restoring native ecosystems. Less fertilizer also translates to less energy used.

1.2 Thesis contributions

This thesis aims to provide insight into triuret metabolism in nature: the enzymes that are involved, their mechanisms, the regulation of the encoding genes and the scope of the

metabolism in the microbiome. The enzyme that degrades triuret (triuret hydrolase) was discovered in this work and the crystal structure was solved. The enzyme mechanism was elucidated and an intriguing comparison was presented with a paralog of the enzyme that breaks down biuret from the same operon. Leading from the discovery of the triuret hydrolase, two more enzymes were discovered that act on the product of triuret hydrolase. These new enzymes are analogs of each other but derive from two different protein folds, one being a metalloenzyme. The regulation of triuret metabolism was found in a *Herbaspirillum* species to have specific upregulation in the presence of triuret, indicating a highly evolved system. With the knowledge of these new enzymes, bioinformatics analysis revealed the entire phylogeny of the triuret hydrolase in recorded genomes. A majority of the genes are found in plant-associated bacteria. The work has opened up several avenues of research including potential fertilizer application, science of the plant-bacterial symbiosis and enzyme evolution.

1.3 Thesis outline

The remainder of this thesis is organized as follows.

- Chapter 2 describes the discovery of the triuret hydrolase involving enzyme kinetics, crystallography and spectroscopy.
- Chapter 3 goes into the regulation of the operon containing triuret hydrolase in the bacterium *Herbaspirillum* sp. BH-1. In addition, the discovery is described of two carboxybiuret decarboxylases that evolved from different protein folds.
- Chapter 4 presents the potential application of triuret as a N fertilizer and obstacles that will need to be overcome. In addition, some concluding remarks are made.

1.4 Notational conventions

1 Unit (U) defined as 1 μmol ammonia per minute at the pH optimum of the enzyme for a substrate; sp. means *species*; E.C - Enzyme Classification; VDW - Van Der Waals Force

Chapter 2

Discovery and structural analysis of a triuret hydrolase from the biuret degradation pathway in *Herbaspirillum sp. BH-1*

2.1 Introduction

Triuret (carbonyl diurea) is an impurity of industrial urea fertilizer (<0.2%) which results in several hundred thousand tons applied worldwide each year on agricultural lands[12]. Triuret has been described in the literature as early as 1870 when it was first synthesized and, although the natural source of triuret is unknown, it has been present in some fresh water amoebas as granules and detected in humans experiencing high oxidative stress[9,10]. Engelhardt et al. had discovered biodegradation of triuret and isolated a *Corynebacterium* species by enrichment but no enzymes had been identified prior to this study[11]. The discovery of the triuret decomposing enzyme (TrtA) was made by examining genomic regions in the vicinity of biuret hydrolase (E.C 3.5.1.84) genes in bacteria[13,14]. The biuret hydrolase (BiuH) is a amidohydrolase that hydrolyzes biuret to allophanate and is part of

the Isochorismatase-like hydrolase (IHL) superfamily with the catalytic triad of a cysteine, aspartate and lysine residues (Figures 2.1,2.2) [14]. Prior to this study, the only known precursor of biuret was cyanuric acid, a metabolite of *s*-triazine compounds mostly comprised of herbicides. However, based on bioinformatics analysis, biuret metabolism appears to be mostly independent of cyanuric acid metabolism [5,13].

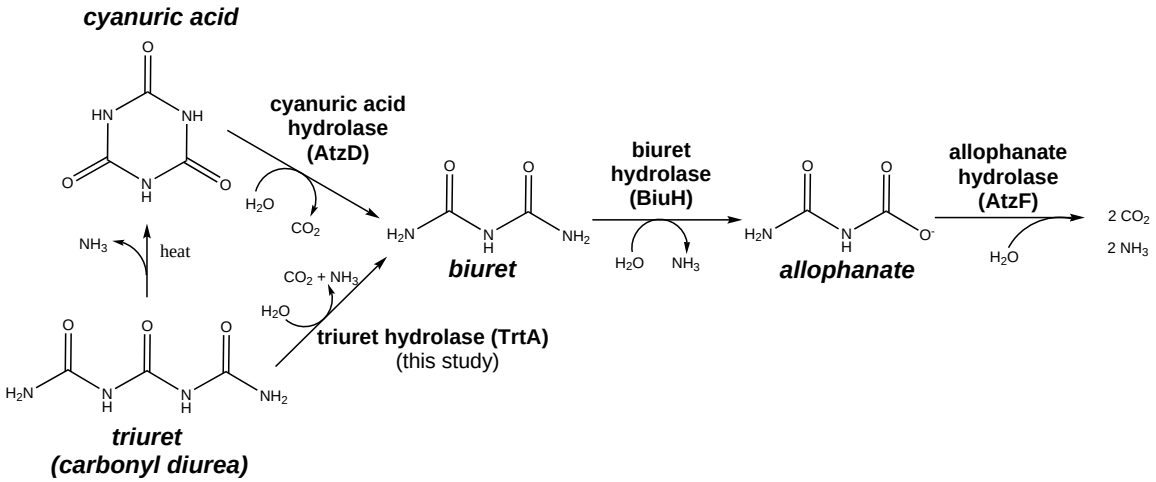

Figure 2.1: Triuret and Cyanuric Acid Mineralization Pathways through Biuret
Pathways are shown through biuret which includes enzymes AtzF, an amidase, AtzD, a metal-dependent amidohydrolase and BiuH,TrtA homologs in the IHL superfamily. Scheme drawn in ChemDraw.

In lieu of the cyanuric acid hydrolase (AtzD) not being in an operon with BiuH, the genome contexts of several hundred BiuH encoding sequences revealed a co-occurring homologous sequence, TrtA, with ∼50% amino acid sequence identity on average but showing no activity on biuret. Interestingly, the active sites of TrtA and BiuH are almost identical in sequence and so it was then hypothesized that triuret be the substrate for TrtA and feed into biuret metabolism. The TrtA sequence used in this study comes from a bacterial enrichment isolate of a biuret fertilized potato field. The bacterium was named *Herbaspirllum* sp. BH-1 and has ∼48% sequence identity to the crystallized BiuH from *Rhizobium leguminosarum* b.v viciae 3841 [13,14]. Both species have operons that contain TrtA, BiuH and the allophanate hydrolase, AtzF, to utilize all four nitrogens from triuret. Interestingly, TrtA and BiuH sequences come largely from plant-associated bacteria that can nodulate or

are known endophytes and the broader context of this metabolism is still unknown but it is hypothesized to come from oxidative purine or uric acid metabolism [9,11,15]. **In this chapter, TrtA is characterized by substrate specificity, kinetics, crystallography and is compared to BiuH in its ability to discriminate triuret from biuret despite their near identical active sites.**

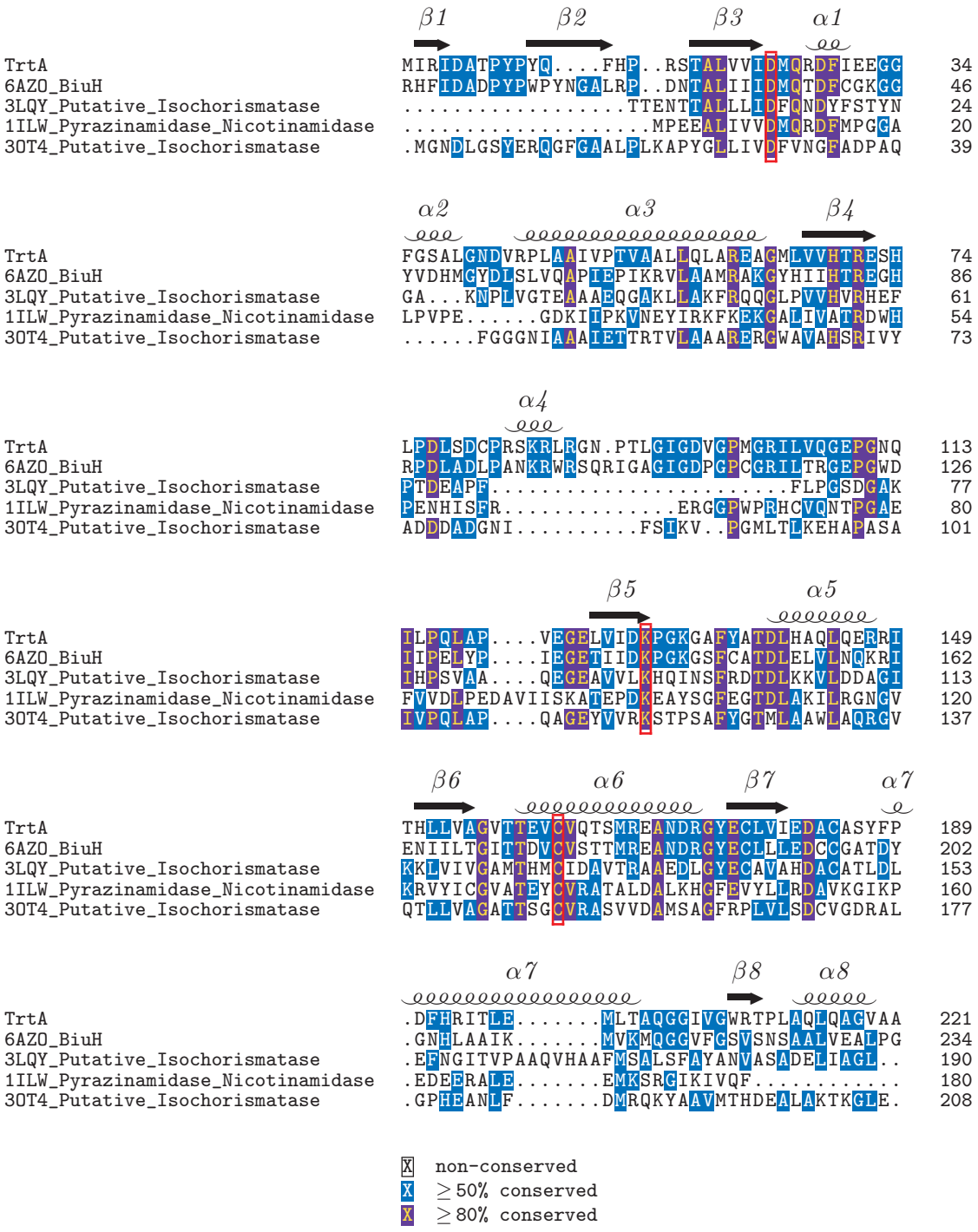

Figure 2.2: Multiple Sequence Alignment of TrtA with BiuH and related IHL Superfamily Members: Sequences are named by PDB ID and aligned using ClustalΩ. Shading of resiudes indicates sequence conservation and the catalytic triad is highlighted in red. Secondary structure annotation denoted for TrtA. Figure created using TexShade

2.2 Methods

Molecular Cloning and Protein Purification

The triuret hydrolase (TrtA) gene from *Herbaspirllium sp. BH-1* (accession no. WP_102661291.1) was codon-optimized and cloned with a N-terminal 6x HisTag and thrombin cleavage site into a pET28a vector using NdeI and HindIII restriction sites and transformed into BL21DE3 E. coli cells (New England Biolabs)[13]. Site-directed mutants and a C-terminal Δ7 deletion were made using the Q5 Site Directed Mutagenesis Kit from New England Biolabs. The *trtA* gene was expressed by growing cells in lysogeny broth (LB) medium with 50 μg/mL kanamycin at 37^{o}C and 200rpm to an OD_{600} of 0.6 in a shake flask. It was then cooled to 16^{o}C and induced with 0.5 mM isopropyl β-D-1-thiogalactopyranoside (IPTG) and with the same agitation incubated for 20 hrs. The cells were then harvested by centrifugation at 1,500xg for 20 min and then resuspended in lysis buffer (20mM sodium phosphate, 0.5 M sodium chloride, 10 mM beta-mercapatoethanol pH 7.4). The cells were then lysed by French Press with three passes at 10,000 psi and the lysate then clarified by centrifugation at 20,000xg for one hour. The triuret hydrolase was purified from the lysate by using fast protein liquid chromatography (FPLC) and Ni-NTA chromatography. Using a GE AKTA FPLC and a GE HisTrap 5mL column, TrtA was purified after running an imidazole gradient from 100 mM to 500 mM and fractions collected. The expression yield for TrtA was 30 mg per liter culture while for a C-terminal deletion mutant the yield was 70 mg per liter culture. Pooled fractions were either buffer exchanged into buffer containing 20 mM sodium phosphate, 200 mM sodium chloride and 10 mM beta-mercapatoethanol at pH 8 for kinetic experiments or into 50 mM Tris, 200 mM sodium chloride and 10 mM beta-mercaptoethanol at pH 8 for thrombin cleavage and crystallization experiments using a 15-mL Amicon 10kDa Centrifugal filter. TrtA protein concentration was determined using the Bradford method (Bio-Rad Protein Assay). The his-tag was cleaved from TrtA using bovine thrombin protease (Sigma) by adding 2 U thrombin per mg TrtA in a dilute protein solution between 5-10 mg/mL with Tris buffer and the cleavage reaction was placed on a rotator at 4^{o}C for >36 hours. The reaction was then concentrated to 2 mL and cleaved TrtA cleavage product was purified by size exclusion chromatography using the

AKTA FPLC and a GE Healthcare HiLoad 16/600 Superdex 200 pg column. The column was equilibrated with 50 mM Tris 200 mM sodium chloride at pH 8, the sample was injected onto the column, and washed with 1 column volume at 1 mL/min flow rate. TrtA eluted as a homodimer at ∼48 kDa and the preparation was then subsequently used in crystallization experiments.

Crystallography

By vapor diffusion in a 24-well hanging drop crystallization plate, crystal growth was sensitive to changes to the relative humidity. In order to prevent condensation, the air was purged from the wells with compressed nitrogen prior to sealing each well. Crystals grew in a range of conditions between 20-30% PEG 6000 (wt/v) and 0.1 M Bis-Tris propane pH 7.5-8.5 in drops of 1μL of protein (10-20 mg/mL) with 1 or 2μL of precipitant. Crystals appeared after one day as orthorhombic crystals and were harvested by looping them into cryoprotectant (mother solution containing 25% v/v ethylene glycol) and frozen in liquid nitrogen. Diffraction data was collected using the Advanced Photon Source (Argonne, Illinois, USA) with various beamlines (Table 2.3). Data was processed using XDS (Build January 26, 2018) and molecular replacement, refinement was done using CCP4 (Version 7.0) and Coot (v0.8.9)[16,17,18]. For molecular replacement the structure of the biuret hydrolase from *Rhizobium leguminosarum b.v viciae 3841* was used (PDB 6AZQ) with 48% sequence identity[14].

Enzyme Kinetics and Spectroscopy

Rate of substrate hydrolysis was determined by ammonia release via the Berthelot Assay. The Berthelot reagent had solution A (1% phenol 50 mg/L sodium nitroprusside) which was added to sample containing ammonium and then solution B (0.5% sodium hydroxide, 0.89% bleach) was added to produce a color response and absorbance was measured at 630 nm. If a substrate interfered with the Berthelot reagent the Ammonia Assay Kit (Sigma) was used which involved adding glutamate dehydrogenase and measuring NADPH disappearance by absorbance at 340nm when α-ketoglutarate is aminated by ammonia to form glutamate. One unit of activity (U) was defined as one micromole substrate per minute at the enzyme's pH optimum at 25^{o}C. Circular dichroism was used to determine the T_m of TrtA with the

Jasco J-815 CD with a 100 μM sample in 20 mM sodium phosphate, 0.2 M sodium chloride pH 8. The temperature gradient was from 55-90^{o}C at a rate of 1^{o}C/min and wavelength set to 220nm. ^{13}C NMR experiments using ^{13}C labeled triuret were conducted using the Varian Unity Innova 400 and VnmrQ 2.2 software.

Chemical Syntheses and HPLC

Biuret (Sigma), 1-nitrobiuret (Sigma), formylurea (Acros), acetylurea (Alfa Aesar) and N-(chloroacetyl)urea (Life Chemicals) were all obtained with high purity (>97%). As triuret is an impurity of biuret (<3% by weight), HPLC was used to quantify the concentration of triuret in biuret solutions using a C18 reversed phase method as developed by Kim *et al*[9].

Triuret: Pure triuret was obtained by oxidation of uric acid with hydrogen peroxide in aqueous ammonia as developed previously by Veneable *et al* with an ∼10% yield[15]. Melting point 236^{o}C, ^{1}H NMR (dmso-d^6): δ 6.90 (br, 2H), 7.25 (br, 2H), 9.65 (br, 2H)

^{13}C labelled Triuret: ^{13}C triuret was synthesized from ^{13}C urea (Sigma) and hydrogen chloride as described in the patent from Scholven Chemie[3]. ^{13}C NMR (100 MHz, dmso-d^6): δ 152.6, 153.8

Methylene diurea: Methylene diurea was synthesized from urea and formaldehyde as developed by Murray *et al*[19]. It contained an insoluble impurity, dimethylene triurea. ^{1}H NMR (dmso-d^6): δ 4.2 (t, 3H, J = 1.2 Hz), 5.65 (br, 4H), 6.48 (br, 2H).

Ethylidene diurea: Ethylidene diurea was synthesized from urea and acetaldehyde as described by Ogata *et al*[20]. ^{1}H NMR (dmso-d^6): δ 1.25 (d, 3H, J = 1.2 Hz), 5.0 (m, 1H, J = 1.2 Hz), 5.65 (br, 4H), 6.3 (br, 2H).

2.3 Results

TrtA is a triuret hydrolase that hydrolyzes triuret to form carboxybiuret.

TrtA kinetics and substrate specificity

TrtA has an apparent molecular weight of 24 kDa and a T$_m$ of 65^oC (Supp. Fig. A.1). Michealis-Menten kinetics were obtained for TrtA from *Herbaspirllium sp. BH-1* which has

a catalytic efficiency (k_{cat}/K_M) of 6.1×10^5 ($M^{-1}s^{-1}$) (Table 2.1). The pH optimum of the enzyme was dependent on the cleavage of the his-tag, increasing from pH 6.5 to pH 8 when cleaved. A C-terminal his-tag was used initially but this form was less active and produced aggregates and instead an N-terminal His-tag was used. To remove a possible intrinsically, disordered region, a C-terminal deletion was made for crystallographic purposes which a multiple sequence alignment of TrtA sequences revealed it to be not common among TrtA proteins. This deletion mutant had negligible effect on the activity of the enzyme but did increase the expression yield by more than 2-fold. TrtA is very specific for triuret as no other substrate tested had more than 0.5% of the activity observed for triuret (Table 2.2). Formylurea and 1-nitrobiuret had more activity over biuret and non-planar compounds ethylidene diurea, methylene diurea and succinamide showed no activity.

Table 2.1: Enzyme Kinetics of TrtA

Variant	pH_{opt}	K_M (μM)	k_{cat} (1/s)	k_{cat}/K_M ($M^{-1}s^{-1}$)
TrtA	6.5	20.5±2.5	11.0±0.4	$5.3\pm1.0\times10^5$
+CleavedHis	8	14.5±2.6	8.8±0.4	$6.1\pm1.6\times10^5$
CtermDelΔ7+CleavedHis	8	16±2.4	10±0.4	$6.3\pm1.3\times10^5$

Table 2.2: Substrate Specificity of TrtA

Substrate	V_{max} (U/mg)	Specificity Ratio
Triuret	24	1
Formylurea	0.07[a]	3.4×10^2
1-nitrobiuret	0.002[a]	1.2×10^3
Biuret	0.0004	6×10^4
Acetylurea	0.0001	1.5×10^4
Tetrauret, pentauret	n.d	
Ethylidene diurea, methylene diurea	n.d	
Succinamide	n.d	

[a] measured by Ammonia Assay Kit

n.d− not detected

Detection of carboxybiuret by ^{13}C NMR

Ammonia release of triuret by TrtA was found to be through carboxybiuret as it was observed by ^{13}C NMR along with biuret and carbonate when labeled ^{13}C triuret was hydrolyzed by the enzyme (Figure 2.3). The decarboxylation of carboxybiuret to biuret was spontaneous with a half-life of around 20 minutes.

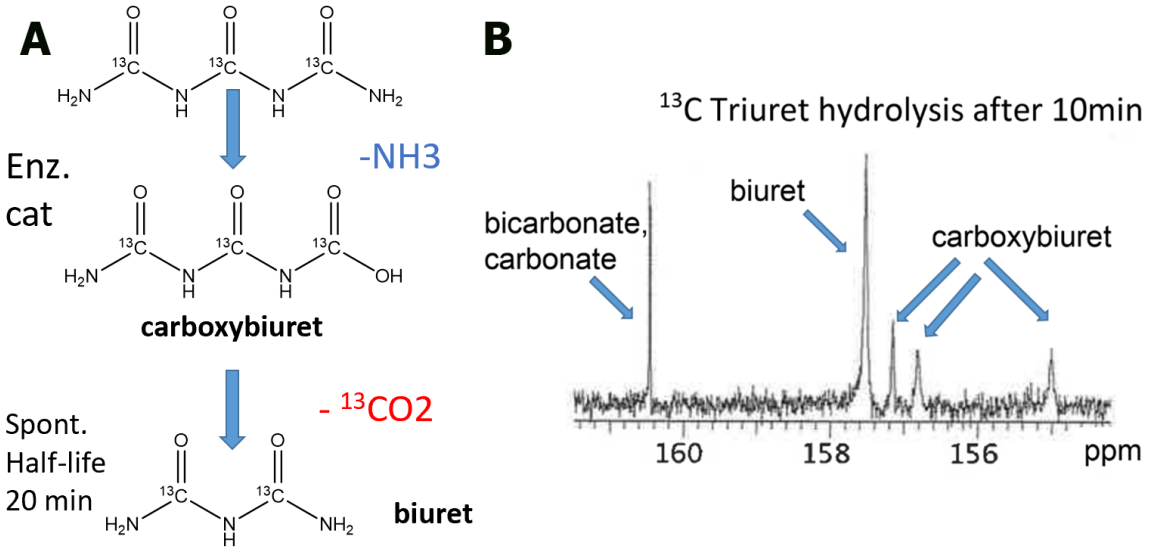

Figure 2.3: Elucidation of the Reaction Product of TrtA by ^{13}C NMR:
(A) Pathway for the fate of triuret hydrolysis with TrtA to make carboxybiuret and then the spontaneous decarboxylation to form biuret. (B) ^{13}C NMR of labeled triuret hydrolysis by TrtA. ^{13}C triuret (∼50mM) was added to 120μM TrtA in 125mM phosphate buffer pH 8 and stirred for a few minutes before doing NMR acquisition which totaled to 10 min incubation.

Overall structure of TrtA

Crystals obtained of TrtA had a maximum size of 0.4 X 0.1 X 0.05 mm and were either in the space group P1 for the apo form or $P2_12_12_1$ for the co-crystals with triuret or biuret (Table 2.3).The apo form made small, fragile crystals on average while the dead mutant of TrtA, co-crystallized with triuret or biuret, was able to make larger, more robust crystals for diffraction. In the asymmetric unit of the apo crystal, with P1 space group, there are four homodimers present. For the co-crystals, both with space group $P2_12_12_1$ and the same unit cell parameters, have two homodimers in the asymmetric unit. TrtA elutes as a dimer by size exclusion chromatography and the monomer adopts a fold typical of the IHL superfamily with six parallel β sheets alternating with six α helices (Rossmann-like) in addition to a two strand antiparallel β sheet at the N-terminus (Figure 2.4) [21]. Helices α6 and α7 provide most of the interactions between the two subunits in the dimer while α4 also has some contact at the interface (Figure 2.5). The α2 helix shows the highest B-factor in the apo crystal and undergoes a significant conformational change (∼4.5$\AA$) when triuret or biuret is bound in the active site.

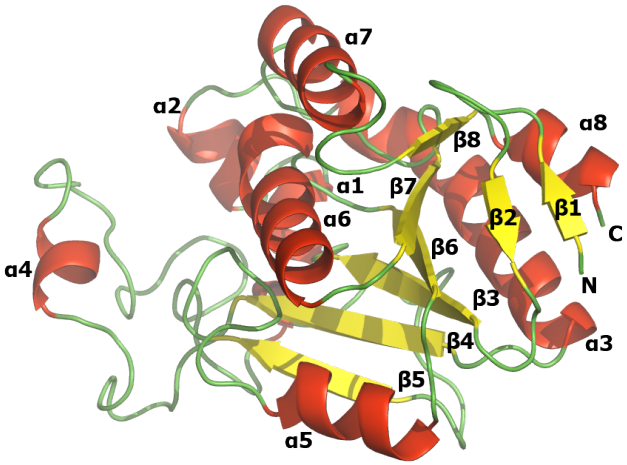

Figure 2.4: Topology of TrtA
Cartoon representation of a monomer structure: Loops are colored green, α helices are in red and β sheets are in yellow. N and C termini are labeled N and C, respectively. Model generated in PyMOL.

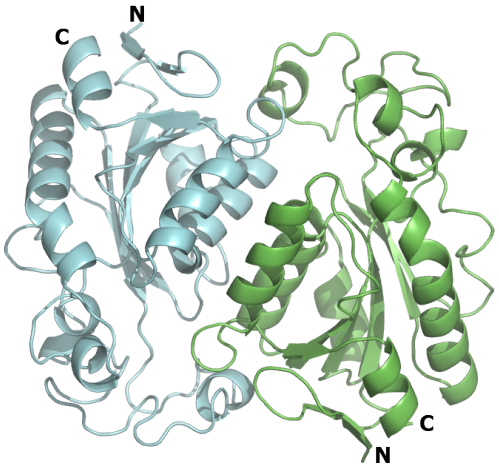

Figure 2.5: TrtA Dimer Structure
Cartoon representation of the TrtA dimer: N and C termini are labeled N and C, respectively. Model generated in PyMOL.

Table 2.3: Summary of X-ray Data Collection and Refinement

Crystal	WT	C162S + 1mM Triuret	C162S + 30mM Biuret
Data collection			
Beamline	24-ID-E	23-ID-D	23-ID-B
Space Group	P1	$P2_12_12_1$	$P2_12_12_1$
Dimension a, b, c ($\AA$)	72.95, 76.55, 93.59	51.53, 114.44, 142.93	51.63, 114.18, 141.47
Dimension α, β, γ (^{o})	118.40, 89.61, 103.07	90.00	90.00
Resolution ($\AA$)	81.57−2.10(2.20−2.10)[a]	60.62−1.45(1.55−1.45)[a]	57.09−1.78(1.88−1.78)[a]
No. observed reflections	194240 (26162)	1121865 (194223)	594818 (88093)
No. unique reflections	91216 (12132)	150183 (26952)	154547 (23387)
R_{merge} (%)	6.8 (17.6)	5.1 (54.7)	6.2 (36.9)
I/σ	9.16 (4.76)	20.99 (3.97)	12.44 (4.26)
Completeness (%)	90.4 (92.2)	100 (100)	99.8 (99.9)
Redundancy	2.13 (2.16)	7.47 (7.21)	3.85 (3.77)
Refinement			
Resolution ($\AA$)	2.10	1.45	1.78
R_{work}/R_{free}	0.1781/0.2267	0.1708/0.1894	0.1637/0.1921
No. atoms			
Protein	13451	6819	6756
Ligand/Ion	32	48	27
Water	818	411	433
Mean B-factors ($\AA^2$)	21.9	21.6	29.3
R.m.s deviations			
Bond lengths ($\AA$)	0.009	0.016	0.007
Bond angles (^{o})	1.56	2.00	0.91
Ramachandran plot (%)			
Core	97.05	98.58	98.58
Allowed	2.37	0.95	0.95
Dissallowed	0.58	0.47	0.47

[a] Numbers in parentheses refer to the highest-resolution shell

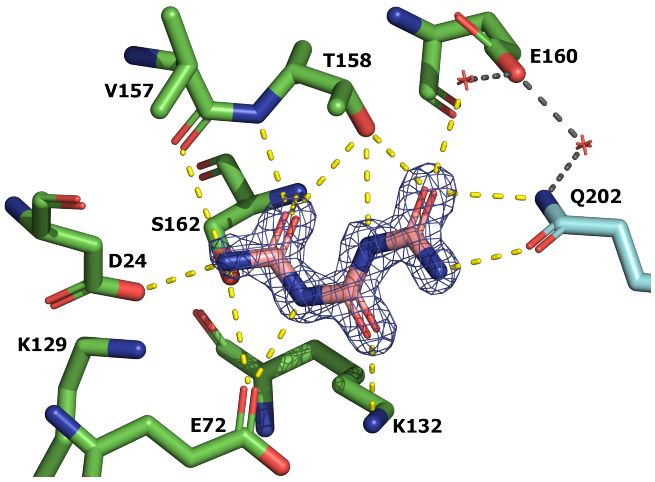

Figure 2.6: TrtA Active Site with Triuret:
2Fo-Fc map for triuret co-crystallized with TrtA contoured at 3σ. Residue color indicates which chain the residue is from. Polar contacts made with the substrate are marked by yellow dash while those coordinating the water molecules shown with dark gray dashes.

Active site of TrtA

The catalytic triad defined by the cysteine hydrolase superfamily are present in TrtA with Asp_{24}, Lys_{129} and Cys_{162} and there is also a *cis*-peptide bond in the active site between residues Val_{157} and Thr_{158} which is signature of the IHL protein family [21]. The active site is complemented by a few residues from the other subunit in the dimer, specifically Gln_{202} that comes from the $\alpha 7$ helix which coordinates biuret and triuret in bound structures. In the apo WT structure, beta-mercapatoethanol (BME) was found covalently attached to the catalytic cysteine of every subunit (Supp. Fig. A.2). The enzyme was inactivated by a Cys_{162}Ser mutation and this allowed for occupancy of biuret and triuret within the active site. In the triuret co-crystal with all four active sites occupied, the substrate makes several hydrogen bonds with residues Asp_{24}, Glu_{72}, Lys_{132}, and as mentioned previously, by Gln_{202} from the other subunit and hydrogen bonds with the backbone amide from the *cis*-peptide bond (Figure 2.6). Triuret also has a polar contact with a water molecule coordinated by Thr_{158} and Glu_{160} and the latter residue also coordinates another water molecule with Gln_{202}. The planarity of the triuret in the active site is distorted as the terminal ureide closest to the catalytic residues is bent with an average torsion angle of 35^o while the other torsion is fairly planar still at 4.5^o on average (Figure 2.8). This

appears to be a pre-attack conformation and triuret in this crystal is in a different conformation compared to the crystal structure of pure triuret [6]. As seen in Figure 2.7, triuret in the active site of TrtA appears to be in a *cis* conformation that allows for a intramolecular H-bond from a middle nitrogen to the terminal carbonyl closest to the catalytic residues. This is not observed in the crystal structure of pure triuret where it is in the *trans* conformation and intramolecular hydrogen bonds are from the terminal amines to the central carbonyl. The *trans* conformation is more stable than the *cis* conformation although the latter is able to pack better into a crystal as it can make more intermolecular hydrogen bonds [6].

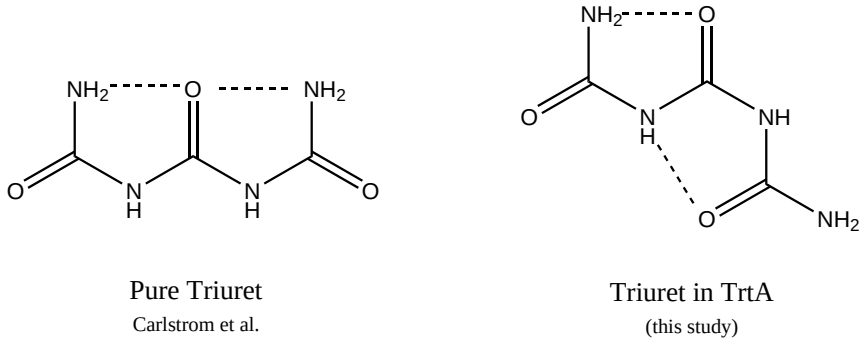

Figure 2.7: Comparison of Triuret structure in TrtA with Pure Triuret:
The structure of pure triuret is in the *trans* conformation while triuret in the TrtA active site is perturbed and has a intramolecular hydrogen bond with a middle nitrogen to a terminal carbonyl. Hydrogen bonds drawn as dashes. Figure drawn using ChemDraw.

Open-Closed Conformations of TrtA

The $\alpha 2$ helix (residues $35 - 39$) undergoes a conformational change when bound with biuret or triuret. The closed conformation is observed in all of the chains of the triuret cocrystal as well as for a single chain in the biuret cocrystal which has biuret bound. The other chains in the biuret cocrystal that do not have biuret bound as well as the apo WT crystal are in the open conformation. Key residues that come into proximity of the active site from the $\alpha 2$ helix are Phe_{35} and Asn_{41} which the former moves $\sim 5\mathring{A}$ and has Van Der Waals Force(VDW) interaction with the substrate with the latter having a hydrogen bond with Gln_{202} (Figure 2.8). Another residue that changes conformation slightly is Phe_{29} which closes in to the substrate by VDW interaction. The active site tunnel is quite large

in the open conformation and is almost nonexistent in the closed conformation of TrtA (Figure 2.9). This phenomenon of open-closed conformation has not been observed in any other members of the IHL superfamily, including the close homolog BiuH.

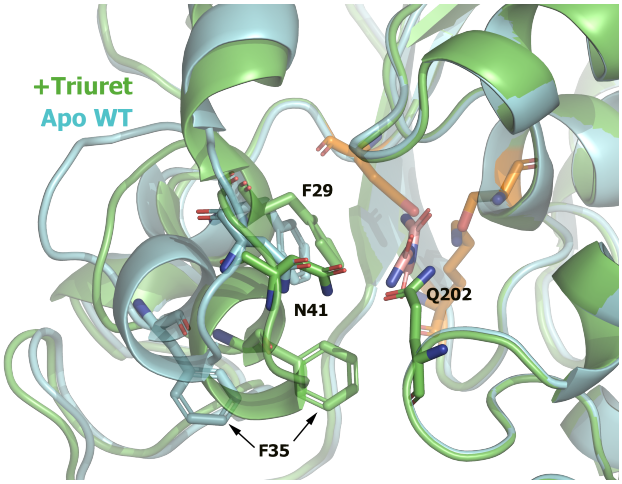

Figure 2.8: Open-Closed Conformations of TrtA:
TrtA cocrystal with triuret overlaid with TrtA apo WT. Triuret and the catalytic triad are colored in light red and orange,respectively. Model generated in PyMOL

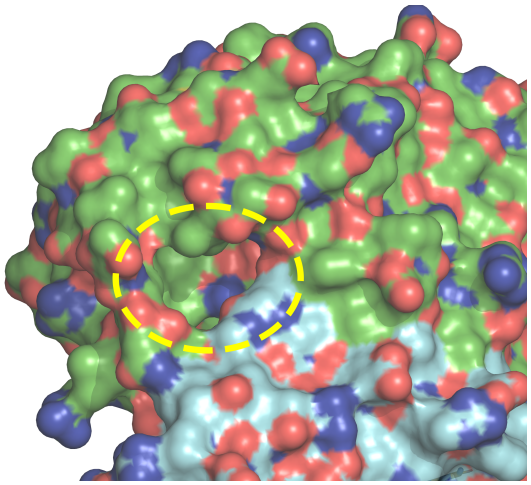

Figure 2.9: Active site tunnel of TrtA:
Surface representation of TrtA apo WT. Active site tunnel labeled with yellow dashes. Model generated in PyMOL

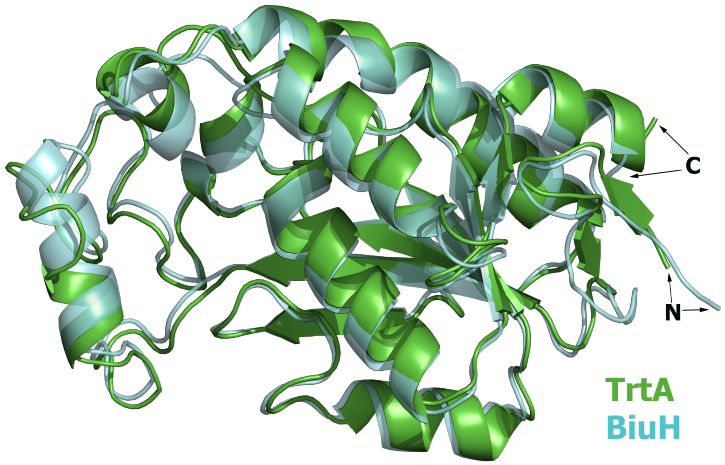

Figure 2.10: TrtA, BiuH Overall structure comparison
Cartoon representation of TrtA overlaid with BiuH (PDB 5BK6). N and C termini are labelled with arrows. Model generated in PyMOL

Comparison of TrtA and BiuH structures

The structure and sequence of TrtA is very similar to the biuret hydrolase structure that was used in phasing which forms a tetramer. The few differences are the loss of the two-strand β sheet (β1 and β2) at the N-terminus and the elongation of the α4 helix in the biuret hydrolase (Figure 2.10). In the active site, almost all of the residues are conserved between TrtA and BiuH with the major difference being the position of the Gln_{202} residue which for BiuH (Gln_{215}) is farther inside the active site by $\sim 2.5\mathring{A}$ (Figure 2.11). Triuret and biuret bound in their respective hydrolases align very closely with similar dihedral angles and make the same hydrogen bonds while triuret has an additional polar contact with a water molecule coordinated by the Glu_{160} residue which in BiuH by consensus is an aspartate.

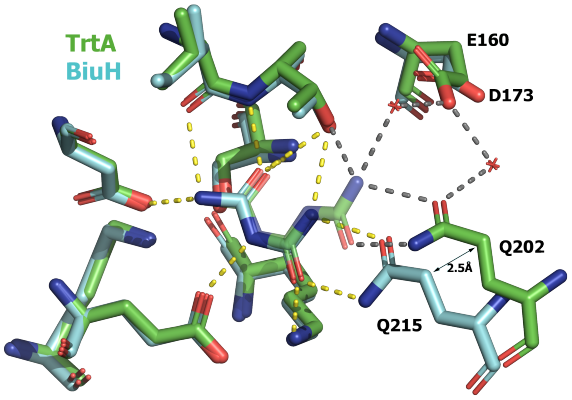

Figure 2.11: Active site comparison of TrtA and BiuH
Model of co-crystallized TrtA with triuret colored in green overlaid with BiuH bound with biuret colored in cyan (PDB 6AZQ). Hydrogen bonds made by biuret are represented as yellow dashes while those only relevant to triuret are shown as dark gray dashes. Key water molecules are represented as red crosses. Model generated in PyMOL

Biuret inhibition of TrtA

Activity on biuret for TrtA is very small but biuret itself is a very weak inhibitor of TrtA. The co-crystal containing biuret, at a concentration of 30 mM biuret, only occupied one of four active sites in the unit cell. Biuret is coordinated by a subset of the residues that coordinate triuret and binds in a non-catalytic fashion (Figure 2.12). The dihedral angle for biuret is fairly planar in this structure and binds in the same place where triuret is planar as well. Preliminary data suggests that biuret is a competitive inhibitor but since biuret contains a 1% (wt) impurity of triuret, the K_M is difficult to determine at the high biuret concentration required to inhibit the enzyme and at higher concentrations of biuret (>50mM) TrtA precipitates as it appears to be a chaotrope. There were attempts to crystallize the active WT with biuret but the crystals formed were very small like the apo form and soaking experiments with biuret resulted in cracking of the crystals. More success was obtained with the C162S dead mutant that made large cocrystals with biuret. This was perhaps due to the BME covalently attached to the catalytic cysteine or the hydroxyl group of the serine making a stronger hydrogen bond than the thiol group of the catalytic cysteine (Supp. Fig. A.2).

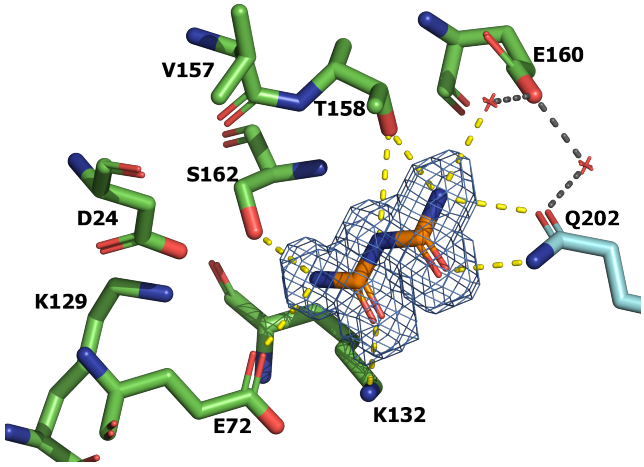

Figure 2.12: TrtA Active Site with Biuret
2Fo-Fc map for biuret co-crystallized with TrtA contoured at 1σ. Residue color indicates which chain the residue is from. Polar contacts made with biuret are marked by yellow dash while those coordinating the water molecules shown with dark gray dashes.

Active site mutagenesis of TrtA

Critical activity-determining residues in the active site of BiuH for were investigated by Esquirol *et al.* They are largely conserved in TrtA and correspond to the residues Asp_{24}, Phe_{29}, Lys_{129}, Lys_{132} and Gln_{202} [14]. To expand the scope of residues critical for triuret activity and to identify the mechanism of how triuret and biuret are discriminated the residues in consensus between TrtA and BiuH were mutated. The positions were Phe_{35}, Leu_{39}, Asn_{41}, Glu_{160}, Tyr_{187}, Ile_{205} and Ala_{134} (Figure 2.13). The residues Phe_{35}, Asn_{41} and Tyr_{187} lie at the entrance to the active site while Glu_{160} and Leu_{39}, Ile_{205} interact with Gln_{202} by a H-bond network, for the former, or by VDW interaction for the latter two residues. Ala_{134} is positioned behind the catalytic Cys_{162} residue in the core of chain and while all the residues around this alanine are conserved in both TrtA and BiuH, the alanine alone is by consensus in BiuH a serine residue. The mutagenesis strategy was to mutate the residues in TrtA to the consensus mutation in BiuH but since some positions have a backbone that do not align in TrtA with BiuH, a more rational design approach was taken for the residue Leu_{39} that was substituted to an alanine instead.

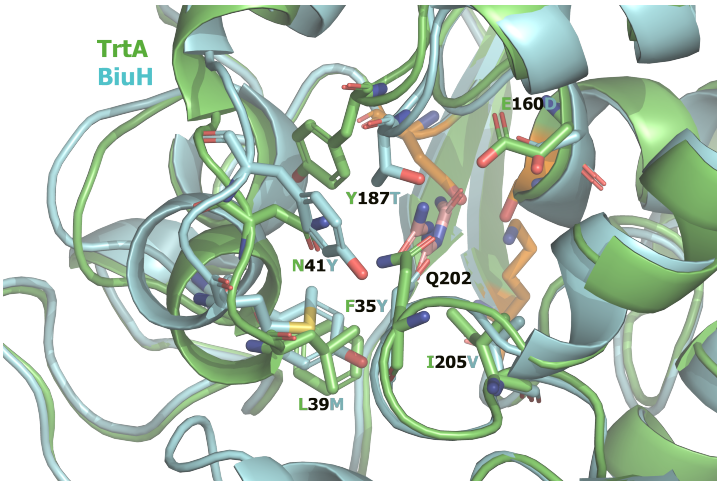

Figure 2.13: Active Site mutagenesis of TrtA:
TrtA cocrystal with triuret overlaid with BiuH (PDB 6AZQ). Select TrtA residues are shown with the BiuH consensus at those positions. Residue labels indicate the position and the BiuH consensus mutation. Triuret and the catalytic triad are colored in light red and orange,respectively.

All of the positions except for Leu_{39} and Ile_{205} have been mutated thus far in TrtA and of those mutated, the majority were deleterious to triuret activity except for A134S (Figure 2.14).The variant E160D had 50% of the maximal activity while single variants F35Y, Q202E, Y187T and N41Y had less than 10%. As mentioned previously, the C162S variant was inactive and used to co-crystallize TrtA with triuret and biuret. No single mutant saw an increase in biuret activity except for Q202E which saw a 10-fold increase but was still three orders of magnitude less than its activity on triuret.

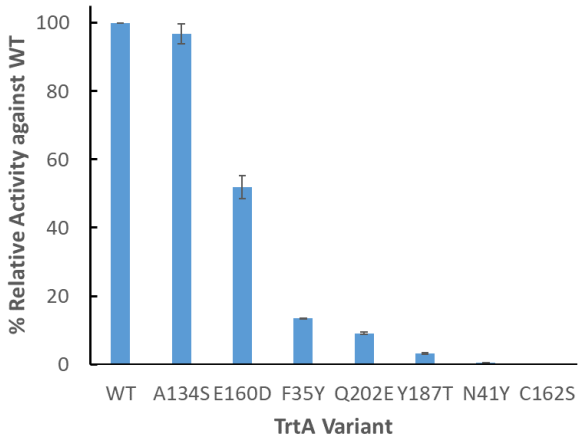

Figure 2.14: Relative Triuret activity of TrtA variants against WT
Variants were purified by Ni-NTA chromatography and activity measured by the Berthelot assay. Error bars indicate one standard deviation of the mean.

2.4 Discussion

TrtA poses an interesting evolutionary question in that it is very specific for triuret; yet the activity on biuret is five orders of magnitude less than on triuret.

TrtA is a native enzyme of triuret hydrolysis

The enzyme has a catalytic efficiency on the order of 10^5 $M^{-1}s^{-1}$ which is typical for enzymes active on natural metabolites [22]. The substrate with weak activity, 1-nitrobiuret, can be considered a stable mimic of the triuret reaction product, carboxybiuret, which it may be inferred that carboxybiuret can be hydrolyzed by TrtA albeit at a very slow rate to make dicarboxyurea, an even more unstable compound. An amidase, not in the IHL superfamily, already exists to hydrolyze carboxybiuret to dicarboxyurea which is named AtzEG and found in the cyanuric acid mineralization pathway of *Pseudomonas* sp. ADP [23]. The enzyme AtzE and AtzF, the latter being an allophanate hydrolase, have a similar relationship like BiuH and TrtA. They are homologs of each other and their native substrates differ by only one additional amide group, although in this case, the active site residues coordinating the substrates are completely different [24]. TrtA is not the only enzyme to generate carboxybiuret. Cyanuric acid hydrolase also produces carboxybiuret

through opening of the ring and a ^{13}C NMR study of this reaction produced very similar results to TrtA by observing carboxybiuret, biuret and bicarbonate/carbonate peaks [25].

Catalytic Mechanism of TrtA

In the IHL superfamily, the catalytic triad is positioned non-linearly, unlike other triads. Instead, IHL enzymes form a more triangular positioning where the acidic aspartate (Asp_{24}) helps stabilize the basic Lys_{129} but also binds the substrate (Figure 2.6). While the catalytic lysine or aspartate can abstract a proton from the catalytic cysteine residue (Cys_{162}), it is the positive charge of the lysine residue that will effectively lower the pKa of the cysteine and make the residue a stronger nucleophile when negatively charged. The loss of planarity of the triuret for the amide moiety near the catalytic triad suggests that this is a pre-attack conformation that is made possible by the negatively charged Asp_{24} and Glu_{72} residues which help create a dipole moment in line with the carbonyl and make the amide have more sp^3 character like the transition state (Figure 2.15).

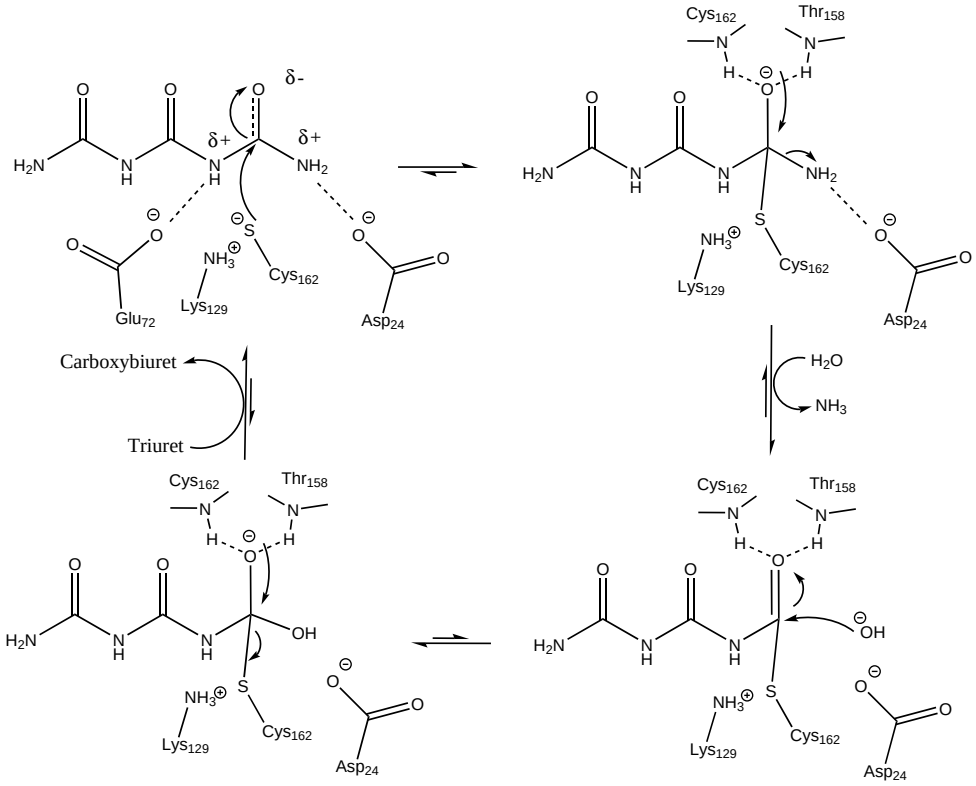

Figure 2.15: Proposed Catalytic Mechanism for TrtA:
The catalytic triad comprises of Asp_{24}, Lys_{129} and Cys_{162} while an additional residue Glu_{72} is drawn for its role in the Michaelis complex. The oxyanion hole is represented by the backbone nitrogen atoms of Cys_{162} and Thr_{158}. Reaction scheme drawn in ChemDraw

When the cysteine nucleophile attacks to make the tetrahedral transition state, the oxyanion hole is formed by the backbone nitrogen atoms of Thr_{158} and from the catalytic cysteine, Cys_{162}. The amine then leaves as ammonia following the formation of the thioester linkage which subsequently is attacked by water to make the second tetrahedral transition state. The active site is then regenerated when carboxybiuret is released with the catalytic cysteine as the leaving group.

Discrimination of Triuret vs Biuret: The role of Gln$_{202}$

While TrtA and BiuH have the same residues to coordinate triuret and biuret, the key difference between the two is the position of the Gln_{202} residue where in BiuH is closer in to coordinate the smaller biuret, and in TrtA, is farther out to accommodate triuret (Figure 2.11). The biuret co-crystallized with TrtA binding in a non-catalytic fashion

suggests that the glutamine residue has a strong role in stabilizing the pre-attack conformation as biuret is fairly planar in this structure (Figure 2.12). Interestingly, Gln_{202} in TrtA does not change conformation in either the open or closed conformations despite it being in a different position in BiuH. Therefore it is second shell residues around this glutamine that can evolve the enzyme to become a triuret or a biuret hydrolase (Figure 2.13). The mutation at Glu_{160} to aspartate removed the coordination of the water molecules that hydrogen bond with triuret and Gln_{202} and led to a 50% loss in activity. Mutations of residues related to the open-closed conformations N41Y, F35Y and Y187T were deleterious to triuret activity perhaps affecting the mobility of the $\alpha 2$ helix which may be crucial in substrate tunneling and product release. The open-closed conformations are not observed in BiuH as this may be a phenomenon only in TrtA to accommodate the larger triuret substrate. Further mutagenesis will shed more light on what makes TrtA a triuret hydrolase and not a biuret hydrolase and the variants that will be investigated are L39A and I205V. The residues Leu_{39} and Ile_{205} prohibit Gln_{202} from being able to move more inside the active site, like in BiuH, by steric hindrance and the residues that fixate this residue at its current position in TrtA are Asn_{41} by hydrogen bonding and via a water molecule, Glu_{160} which mutation of these latter two residues saw deleterious effects to triuret activity (Figure 2.16). The selectivity of the enzyme, favoring triuret heavily, could have a physiologic importance in that biuret is inhibitory to the enzyme and this pressured TrtA to become very selective. Another way to look at this is that the selectivity is a consequence of being efficient on hydrolyzing biuret or triuret. Triuret and biuret may need to be tightly bound in order to be active substrates and this maybe explains the rigidity of the glutamine residue which does not change in either the unbound or bound forms of TrtA.

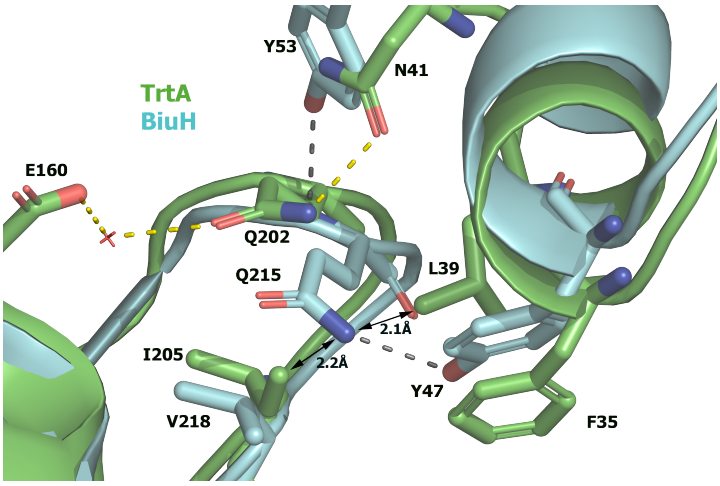

Figure 2.16: Second-Shell residues around the Critical Glutamine Residue in TrtA and BiuH
Polar contacts for the Gln_{215} residue of BiuH (PDB 6AZQ) as dark gray dashes and those for Gln_202 of TrtA (triuret cocrystal) drawn as yellow dashes. A single water molecule is represented as a red cross. Model and distances measured using PyMOL

In BiuH, Asn_{41} is a tyrosine (Tyr_{53}) which may prohibit the glutamine from moving away from the active site like in TrtA but with a valine residue at Ile_{205} (Val_{218}) it can be as close as it is in the active site for which the glutamine residue is then fixated by another tyrosine at the TrtA position of Phe_{35} (Tyr_{47}). There is no observation of open-closed conformations for BiuH but the single conformation that is observed is in a sense a hybrid of the open and closed conformations of TrtA. The backbone of TrtA and BiuH do not overlay exactly in this region so it would not be surprising if mutations from TrtA to the BiuH consensus, or vice versa, would cause deleterious effects to both triuret and biuret hydrolase activities in particular. In conclusion, it seems that the fixation of Gln_{202} in addition to its range of motion is crucial for activity and specificity as it may play a role in stabilizing the pre-attack conformation of biuret/triuret, where the planarity is perturbed for molecules that should have complete delocalisation of electrons.

Chapter 3

Regulation of the triuret degradation pathway in *Herbaspirillum* sp. BH-1: Discovery of carboxybiuret decarboxylation function from two structurally divergent enzymes

3.1 Introduction

Herbaspirillum sp. BH-1 encodes the first ever characterized triuret hydrolase (TrtA) in an operon that mineralizes triuret (carbonyl diurea) completely to ammonia and carbon dioxide (Chapter 2). The bacterium can utilize triuret as the sole nitrogen source in minimal medium and was isolated from agricultural soil by enrichment on biuret, a triuret degradation metabolite. The genome was sequenced by whole-genome shotgun sequencing (RefSeq:GCF_002870055.1) which did not find any nitrogen fixation genes that can be

found in other species of the same genus such as *H. seropedicae*,*H. lusitanum* and *H. frisingense* that are also known endophytes of non-leguminous plants. The triuret degradation pathway in *Herbasprillum* sp. BH-1, which is the predominant pathway in recorded genomes, consists of four enzymatic steps encoded by the genes *trtA*, *trtB*, *biuH* and *atzF* (Figure 3.1). A minority of triuret degraders (∼10% of genomes with *trtA* in RefSeq database) use an alternate pathway (lower in figure) that uses *atzEG* and *atzH* in place of *trtB* and *biuH*. This pathway is also used by the well studied atrazine and cyanuric acid degrading *Pseudomonas* sp. ADP strain. Cyanuric acid hydrolase (AtzD) and triuret hydrolase have the same breakdown product, carboxybiuret, which is fairly unstable and can undergo spontaneous decarboxylation to biuret with a half-life of 20min at pH 8[23]. In *Herbaspirillum* sp. BH-1, however, this decarboxylation is catalyzed by the decarboxylase enzyme encoded by *trtB*, an AtzH homolog, to form biuret(this study). Biuret is then hydrolyzed by biuret hydrolase (BiuH), a homolog of TrtA, to produce allophanate which can then be hydrolyzed by the allophanate hydrolase (AtzF). Allophanate is known to form urea via a slow, non-enzymatic decarboxylation at pH 8, but the rate can increase drastically at lower pH[24].

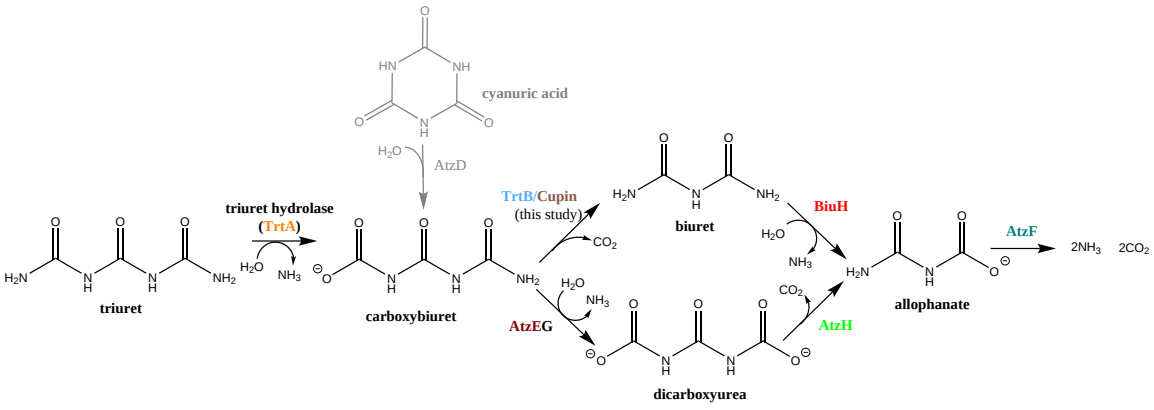

Figure 3.1: Mineralization of Triuret through Biuret and Carboxybiuret:
Triuret and cyanuric acid metabolism can operate by two pathways starting from carboxybiuret. Carboxybiuret is unstable and does decarboxylate spontaneously to biuret (half life 20min). The lower pathway is only ∼10% of TrtA genomes from the RefSeq database. Scheme drawn in ChemDraw.

The *Herbasiprillum* genus is a member of the order Burkholderiales within

betaproteobacteria and previous nitrogen metabolism studies relating to this order have investigated the control of nitrogen fixation by general nitrogen regulatory proteins[26,27,28]. Similar to other proteobacteria, general nitrogen control has been characterized by the genes *glnB*, *glnK*, *glnD*, *ntrB*, *ntrC* and *rpoN*. The genes *glnB* and *glnK* both encode P_{II}-like proteins where the former is consitutively expressed and the latter is expressed under nitrogen starvation conditions and both are subject to reversible uridylylation by GlnD, a uridylyltransferase. GlnD senses the ratio of glutamine to 2-oxoglutarate and has enhanced deuridylylation activity with elevated glutamine levels (ammonium-sufficient) and repressed activity during nitrogen limitation with elevated 2-oxoglutarate levels[29]. The P_{II} proteins can regulate the activity of the phosphatase NtrB on NtrC, a transcriptional activator during nitrogen limitation conditions. The gene *rpoN* codes for RpoN, a σ^{54} factor, which is a unique sigma factor for transcription at promoter sequences activated by NtrC or nitrogen fixation transcription factors[30]. It is of interest to determine if general nitrogen control regulates triuret metabolism as this could indicate a highly evolved system and give insight in what conditions triuret metabolism exist as it is theorized that the source of triuret comes from oxidative uric acid/purine metabolism[7].

All of the nitrogen control genes are present in *Herbaspirillum* sp. BH-1 and in the TrtA operon there is a predicted GntR type regulator from the FadR family, named *trtR* (Figure 3.2). This regulator type has a C-terminal ligand binding domain and a N-terminal DNA binding domain and it is proposed to be involved in the regulation of triuret metabolism[31,32]. An ABC transporter cassette is also in the gene context and is likely to actively transport triuret into the cell.

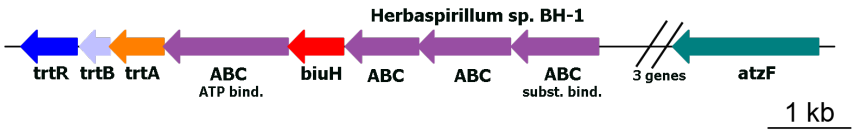

Figure 3.2: Gene Context of TrtA in *Herbaspirillum* sp. BH-1:
Gene context taken around TrtA within in a ±8 gene window using RODEO and visualized using genoPlotR.

The frequency of genomes that have the *trtA* gene in the RefSeq database is less than 1% and within this small percentage is present mainly in bacteria (88%) with probable horizontal gene transfer into plankton (1.2%), chlorophyta (0.7%) and evidence for a TrtA-AtzF fusion in asomycota (9.9%) (Figure 3.3). There are several arrangements of the genomic context for *trtA* in the different clades of the phylogeny that will be discussed in this chapter, one difference in particular can be the substitution of the *trtB* gene for one encoding a Cupin family protein which will be referred to as Cupin. This protein was also found to have carboxybiuret decarboxylase activity and therefore is analogous to TrtB but are structurally divergent to each other (Figure 3.1). **In this chapter, the regulation of the *trtA* operon in *Herbaspirillum* sp. BH-1 is investigated and the decarboxylase function is demonstrated for TrtB and Cupin.**

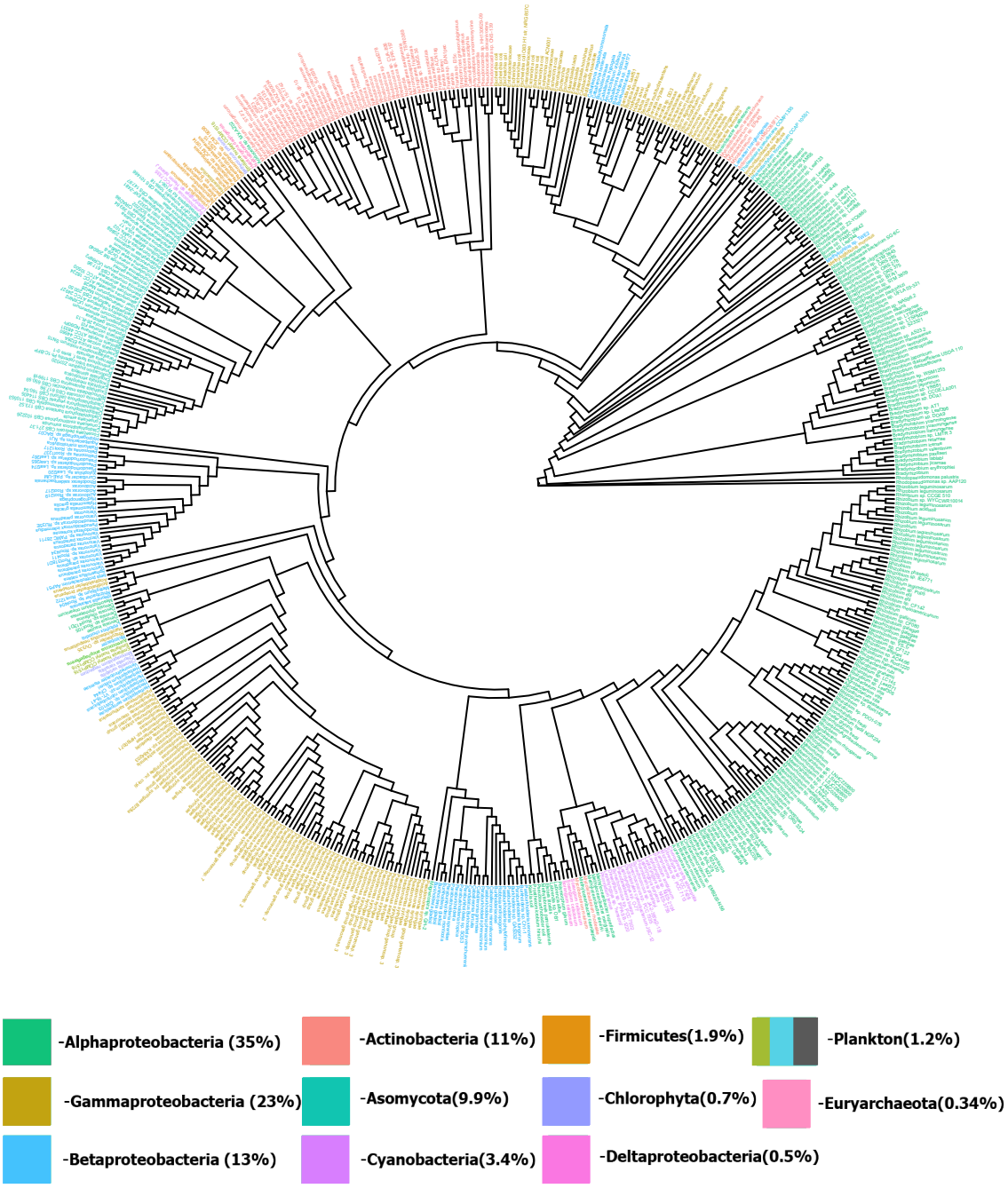

Figure 3.3: Phylogenetic Tree and Taxonomy of Triuret Hydrolase:
Unrooted maximum-likelihood phylogeny of 587 high-confidence TrtA sequences analyzed in this study. Tree generated using RaxML with PROTGAMMAJTT substitution and 1000 bootstrap replicates. Tree visual generated using ggtree package in R programming.

3.2 Methods

Bioinformatics

TrtA sequences were mined from the RefSeq genome database by first generating a sequence similarity network (SSN) using the EFI-EST tool to perform pairwise blast on 10,000 related sequences[33]. Cytoscape was used to visualize the clustering in the SSN and identify the cluster with TrtA sequences[34]. Then, by multiple sequence alignment, the close homologous sequences encoding BiuH were separated from TrtA by evaluating six signature residues (F35, L39, N41, E160, Y187, I205 in TrtA) near the periphery of the active site of both TrtA and BiuH where there is a strict consensus for each enzyme (Chapter 2). This resulted in a total of 587 TrtA sequences. To annotate gene contexts properly, Hidden Markov Models (HMM) were built for TrtA, BiuH, AtzH, TrtB, Cupin, AtzD and the co-occurring major facilitator superfamily (MFS) transporter using HMMER v 3.1b2[35]. These models were then used with the tool RODEO to analyze the gene contexts of the 587 TrtA sequences within a ±8 gene window[36]. The phylogenetic tree was generated using RaxML v 8.2.9 with a PROTGAMMAJTT substitution model and 1000 bootstrap replicates[37].

Induction Assay

To test for the induction of TrtA, BiuH and Urease in *Herbaspirillum* sp. BH-1, the bacteria were grown to late exponential phase overnight in minimal medium (AMS medium) under ammonium sufficient conditions (6mM ammonium chloride) in baffled flasks at 30^{o}C with 250rpm agitation[38]. This culture was then used to inoculate 100 mL cultures in 500mL baffled flasks, to an O.D$_{600}$ of 0.1, that contained minimal medium and nitrogen sources with 4mM of nitrogen. The cultures were then incubated at 30^{o}C with 250rpm agitation and harvested at ∼0.6 O.D. by centrifugation (1500xg for 20 min) and decanting the supernatant. The pellets recovered were stored at -80^{o}C prior further use. Samples were then resuspended in 20 mM sodium phosphate, 0.5M NaCl pH 7.4 buffer at 0.25 g pellet per mL and then were sonicated (20% maximum amplitude, 10 sec on, 10 sec off, 1 min total) before being centrifuged at 20,000xg for 15 min to obtain the clarified lysate. The samples were then assayed for protein concentration by Bradford (Bio-Rad

Protein Assay) and used immediately in kinetics experiments. To measure the expression of triuret hydrolase, allophanate hydrolase and urease, lysates were added to 1mM triuret, potassium allophanate or urea in 125mM sodium phosphate pH 7, 8 or 7.5 buffer, respectively. The rate of substrate hydrolysis was determined by ammonia release via the Berthelot Assay. The Berthelot reagent had solution A (1% phenol 50 mg/L sodium nitroprusside) which was added to sample containing ammonium and then solution B (0.5% sodium hydroxide, 0.89% bleach) was added to produce a color response and absorbance was measured at 630 nm.

Molecular Cloning and Protein Purification

The carboxybiuret decarboxylase gene (TrtB) from *Herbaspirllium sp. BH-1* (accession no. PLY61271.1) and the cupin analog of TrtB, Cupin, from *Rhizobium leguminosarum* b.v viciae 3841 (accession no. CAK10582.1) were codon-optimized and cloned with a N-terminal 6x HisTag and thrombin cleavage site into a pET28a vector using NdeI and HindIII restriction sites and transformed into BL21DE3 E. coli cells (New England Biolabs)[13]. Site-directed mutants were made using the Q5 Site Directed Mutagenesis Kit from New England Biolabs. The genes were expressed by growing cells in lysogeny broth (LB) medium with 50 μg/mL kanamycin at 37^{o}C and 250rpm to an OD_{600} of 0.6 in a shake flask which was then cooled to 16^{o}C and induced with 0.5 mM isopropyl β-D-1-thiogalactopyranoside (IPTG) and with the same agitation incubated for 20 hrs. The cells were then harvested by centrifugation at 1,500xg for 20 min and then resuspended in lysis buffer (20mM sodium phosphate, 0.5 M sodium chloride pH 7.4). The cells were then lysed by French Press with three passes at 10,000 psi and the lysate then clarified by centrifugation at 20,000xg for one hour. The genes were purified from the lysate by using fast protein liquid chromatography (FPLC) and Ni-NTA chromatography. Using a GE AKTA FPLC and a GE HisTrap 5mL column, TrtA was purified after running an imidazole gradient from 100 mM to 500 mM and fractions collected. The expression yield for both TrtB and Cupin was ∼70 mg per liter culture. Pooled fractions were buffer exchanged into 20 mM sodium phosphate 200 mM sodium chloride pH 8 using a 15-mL Amicon 10kDa Centrifugal filter and protein concentration determined by

Bradford (Bio-Rad Protein Assay).

Coupled Enzyme Ammonia Assay

To observe the carboxybiuret decarboxylase function, the assay included either AtzD (from *Moorella thermoacetica* ATCC 39073) or TrtA (from *Herbaspirllium sp. BH-1*) to generate carboxybiuret and BiuH (from *Rhizobium leguminosarum* b.v viciae 3841) to release ammonia from the biuret generated from TrtB or Cupin[13,39]. The rate of ammonia release was then quantified using the Berthelot assay as mentioned in the Induction Assay part of the Methods section. The concentrations used in this coupled assay were 20μg/mL AtzD (or 16μg/mL TrtA) and 4μg/mL BiuH with or without TrtB (40μg/mL) or Cupin (6.2μg/mL) in 1mM cyaunric acid or triuret in 125mM sodium phosphate pH 8. The enzyme concentrations of AtzD and TrtA were calculated to be able to hydrolyze completely cyanuric acid and triuret, respectively, with less than one minute of incubation. Ideally, the rate of ammonia release observed is the steady state hydrolysis of biuret, with the generated carboxybiuret depleted by excess TrtB and Cupin. Cyanuric acid and AtzD became the primary choice of carboxybiuret generation as it does not release ammonia, as like TrtA, which can affect the rate measurement of ammonia produced from biuret hydrolysis.

Metal Analysis and Chelation of Cupin

To determine which metal ions were binding Cupin, a sample was prepared for ICP-OES (Inductively Coupled Plasma-Optical Emission Spectroscopy) by first exchanging the buffer of 25mg Cupin into 20mM Tris-HCl pH8 using an Amicon 10kDa Centrifugal filter. The flowthrough from this filtration was used as a blank and both the protein and the blank sample were then treated with 7%(v/v) nitric acid (Sigma, trace metals grade) and let to digest overnight at room temperature. The samples were then heated to 90^{o}C for 25 min and then spun down to obtain the supernatant which were diluted with DI water to 10mL for a final concentration of 2% v/v nitric acid. Samples were then run on ICP-OES at the Research Analytical Laboratory of the University of Minnesota (St. Paul, MN). To chelate divalent metal ions from Cupin, the enzyme was incubated with 10mM 1,10 phenanthrolein for more than 30 minutes at 4^{o}C which produced a red color.

3.3 Results

Triuret metabolism is in a wide variety of taxa and the gene context around the triuret hydrolase is fairly divergent among bacterial phyla, showing evidence for strong selection pressure with the evolution of carboxybiuret decarboxylase function in two structurally divergent enzymes.

Regulation of triuret metabolism in Herbaspirillum sp. BH-1

Herbaspirillum sp. BH-1 can grow on biuret or triuret as the sole nitrogen source in minimal medium with a doubling time similar to growth on ammonium chloride (∼2.2 hrs). Induction of the triuret degradation pathway appears to be only induced in the presence of biuret or triuret as nitrogenous compounds urea, uric acid, allantoin and nutrient rich medium, lysogeny broth (LB), had no triuret hydrolase activity (Figure 3.4). Urease activity was also assayed to assess if there was a global response to the induction of TrtA and while there was elevated activity from biuret, triuret compared to ammonium-sufficient conditions (ammonium chloride, urea, LB) the same activity was seen with uric acid and allantoin and this could be seen as a nitrogen starvation mechanism. Uric acid and allantoin were tested as it is speculated that the source of triuret comes from oxidative uric acid metabolism. Very small induction of triuret hydrolase may be observed for uric acid but none is found with allantoin.

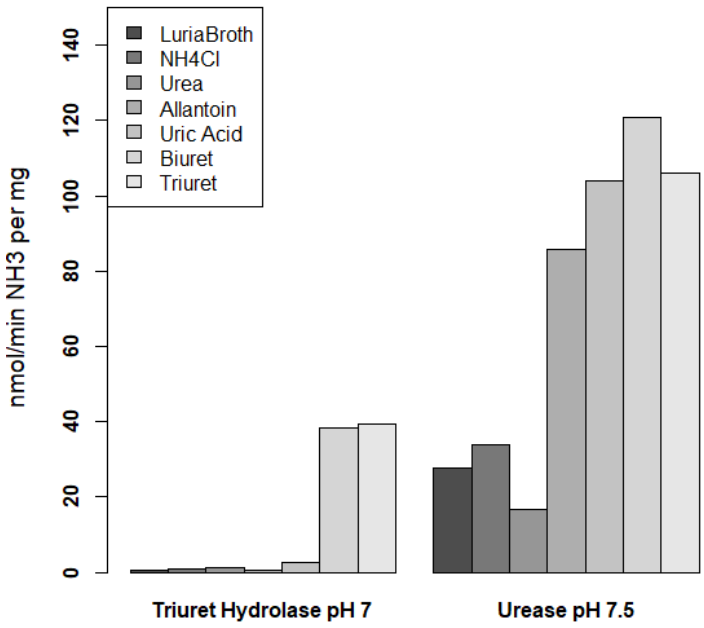

Figure 3.4: Induction of Triuret Hydrolase in *Herbaspirillum* sp. BH-1 grown on Various Nitrogen sources: Activity of lysates on 1mM triuret or urea measuring ammonia release via the Berthelot assay. Lysates were taken from liquid cultures at mid-exponential phase when grown on minimal medium with various sole nitrogen sources. Rates of ammonia release normalized to protein concentration (Bradford). Activity measurements were done in duplicate while cultures were grown in singlicate.

To identify if this induction was triuret or biuret specific and not part of a nitrogen starvation mechanism, serine was used as a sole nitrogen source to simulate nitrogen starvation conditions[40]. In addition, to see whether ammonium-sufficient conditions would suppress triuret metabolism triuret and ammonium chloride were added together as the nitrogen source. The result was that serine alone did not induce the triuret hydrolase and ammonium chloride completely suppressed triuret hydrolase activity (Figure 3.5). The growth of the *Herbaspirillum* sp. on serine alone was very slow compared to the other nitrogen sources and in combination with triuret the growth rate improved. The unexpected result was that serine and triuret together showed significantly reduced triuret hydrolase activity compared to triuret alone despite the ability of triuret to rescue the

simulated nitrogen limitation caused by serine. Urease activity was again induced with triuret along with serine in this experiment to further suggest this response to be related to nitrogen starvation.

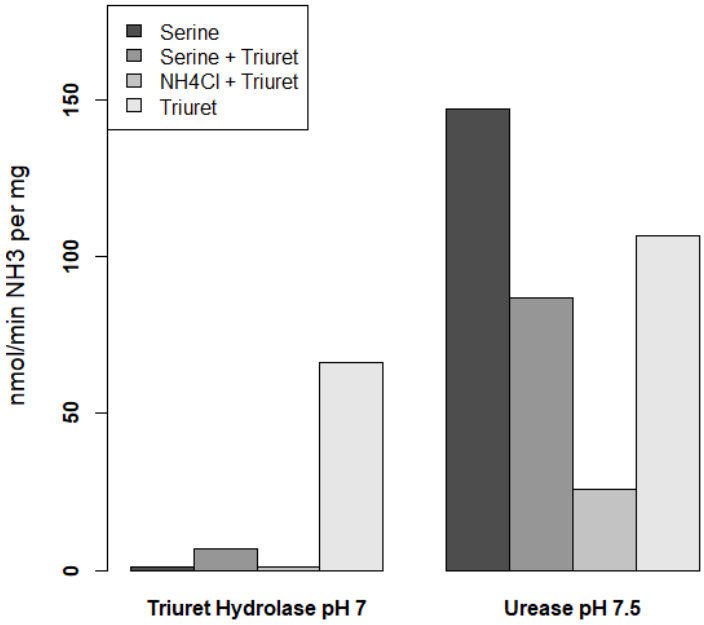

Figure 3.5: Suppression of Triuret Hydrolase in *Herbaspirillum* sp. BH-1 in Starvation and Ammonium Rich Conditions:
Serine was used to simulate nitrogen starvation while ammonium chloride Activity of lysates on 1mM triuret or urea measuring ammonia release via the Berthelot assay. Lysates were taken from liquid cultures at mid-exponential phase when grown on minimal medium with various sole nitrogen sources. Rates of ammonia release normalized to protein concentration (Bradford). Activity measurements were done in duplicate while cultures were grown in singlicate.

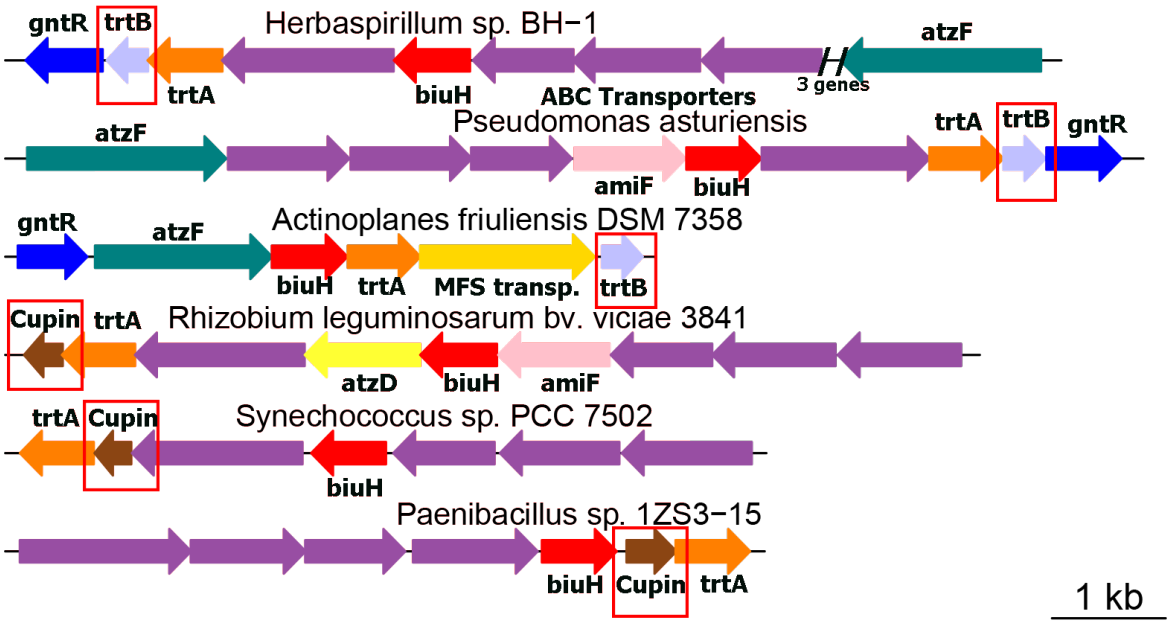

Figure 3.6: Gene contexts around TrtA revealing TrtB and Cupin genes:
TrtB and Cupin are positioned in TrtA gene contexts very similarly and are of similar size but of different protein folds. Both possess carboxybiuret decarboxylase function to produce biuret from carboxybiuret. Gene contexts taken around TrtA within in a ±8 gene window using RODEO and visualized using genoPlotR.

Discovery of Carboxybiuret decarboxylase function of TrtB

The function of TrtB, which is in operon with TrtA and BiuH in *Herbaspirillum*, was inferred based on its homology to AtzH (∼50% identity) to be a carboxybiuret decarboxylase (Figures 3.1,3.2)[41]. AtzH catalyzes the decarboxylation of dicarboxyurea to allophanate (Figure 3.1). A crystal structure exists (PDB 2OWP) for a putative TrtB (∼60% id) from *Burkholderia xenovorans* LB400 which was published by the Joint Center for Structural Genomics (JCSG) with unknown function and aligns structurally very closely to AtzH (rmsd = 0.474$\AA$) with noticeable differences to only two loops proposed to alter substrate specificity as annotated in the sequence alignment below (Figure 3.7).

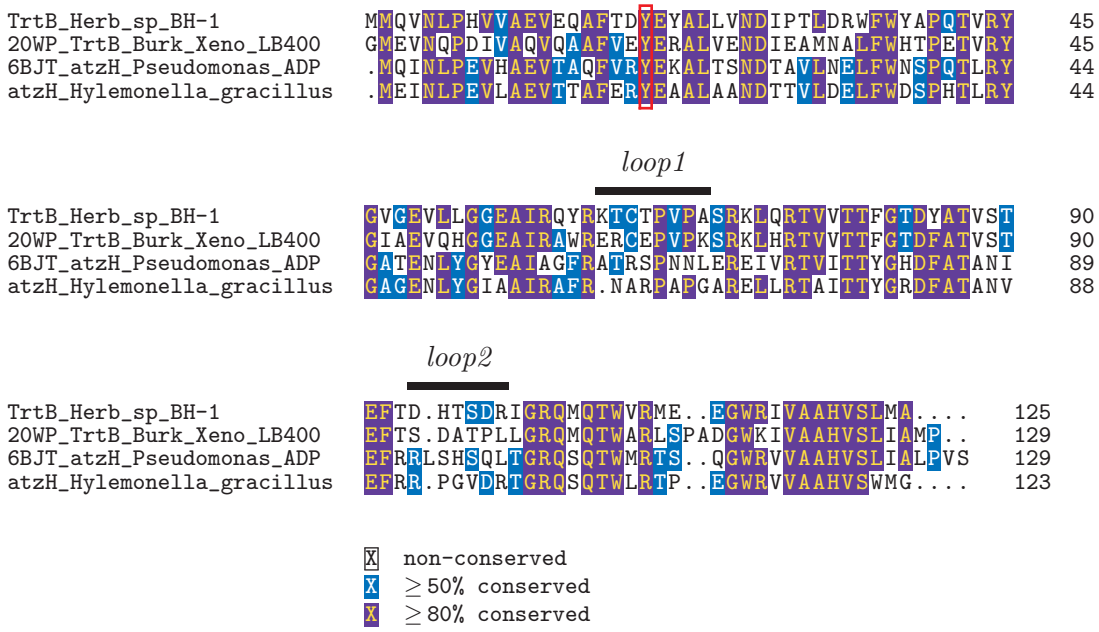

Figure 3.7: Multiple Sequence Alignment of TrtB with AtzH:
Sequences are named by PDB ID when possible and aligned using ClustalΩ. Shading of residues indicates sequence conservation and the catalytic tyrosine is highlighted in red. Figure created using TexShade

The exact residues that bind dicarboxyurea in AtzH are not known as it is not a stable compound to make co-crystals but mutagenesis of the active site tyrosine ($Y_{20}F$) did inactivate the decarboxylase function and the tyrosine is conserved in AtzH and TrtB [41]. The decarboxylase function is observed when coupling TrtB and AtzH with the immediate upstream and downstream enzymes in the pathway. The upstream enzyme generates the substrate for decarboxylation and the downstream enzyme senses the increased steady state concentration of its substrate (over the spontaneous rate of decarboxyation) and thereby releases ammonia at a faster rate than without TrtB or AtzH. As seen in Figure 3.8, TrtA and AtzD both generate carboxybiuret and the addition of TrtB sees a significant, more than two-fold, increase of ammonia release when coupled with BiuH.

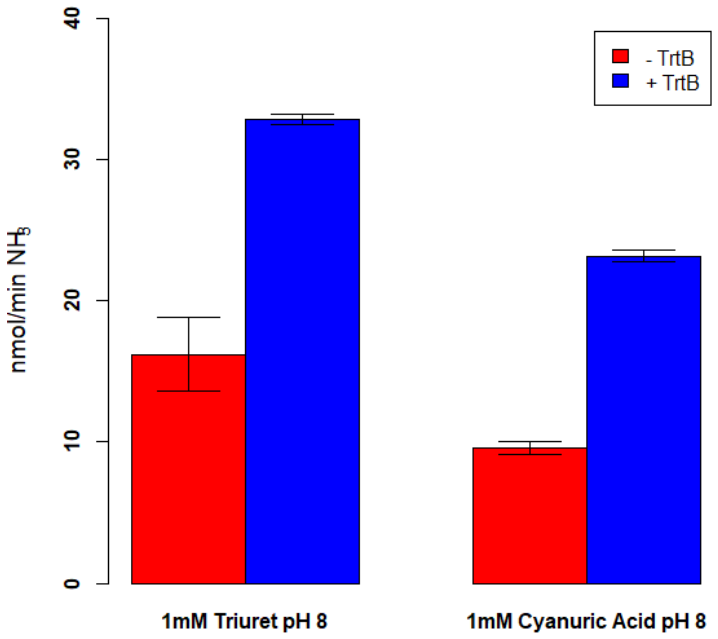

Figure 3.8: Rate Enhancement of Triuret/Cyanuric Acid Mineralisation via TrtB:
The addition of TrtB to a coupled enzyme system containing TrtA and BiuH or AtzD and BiuH enhances the rate of ammonia release measured by the Berthelot assay. AtzD and TrtA both produce carboxybiuret while BiuH hydrolyzes the decarboxylated product, biuret. Error bars indicate one standard deviation of the mean.

Discovery of the function of the Cupin protein: An analog of TrtB

After determining the function of TrtB, the bioinformatics and the gene contexts of TrtA sequences revealed that in lieu of TrtB there is a gene (in an equal proportion of TrtA sequences) that is placed in the same position as TrtB in the gene contexts but has no sequence homology with TrtB (Figure 3.6). Therefore it was inferred that the gene has the same function as TrtB which encodes a protein that is part of the Cupin superfamily, a functionally diverse family that can be enzymes but also transcription factors [42]. Cupin is of similar size to TrtB and characteristic of the Cupin superfamily is a beta barrel fold while TrtB exhibits a Cystatin-like fold which is a beta sheet flanked by alpha helices. The best template to make a homology model from known structures of Cupin proteins

was the 2,4 dihydroxyacetophenone dioxygenase (PDB 5BPX) which has only a 17% sequence identity to the Cupin protein in the TrtA gene context of *Rhizobium leguminosarium* bv. viciae 3841. The sequences of this Cupin and several others revealed that they conserve the metal coordinating residues from the dioxygenase which binds divalent iron (Figure 3.9)[43].

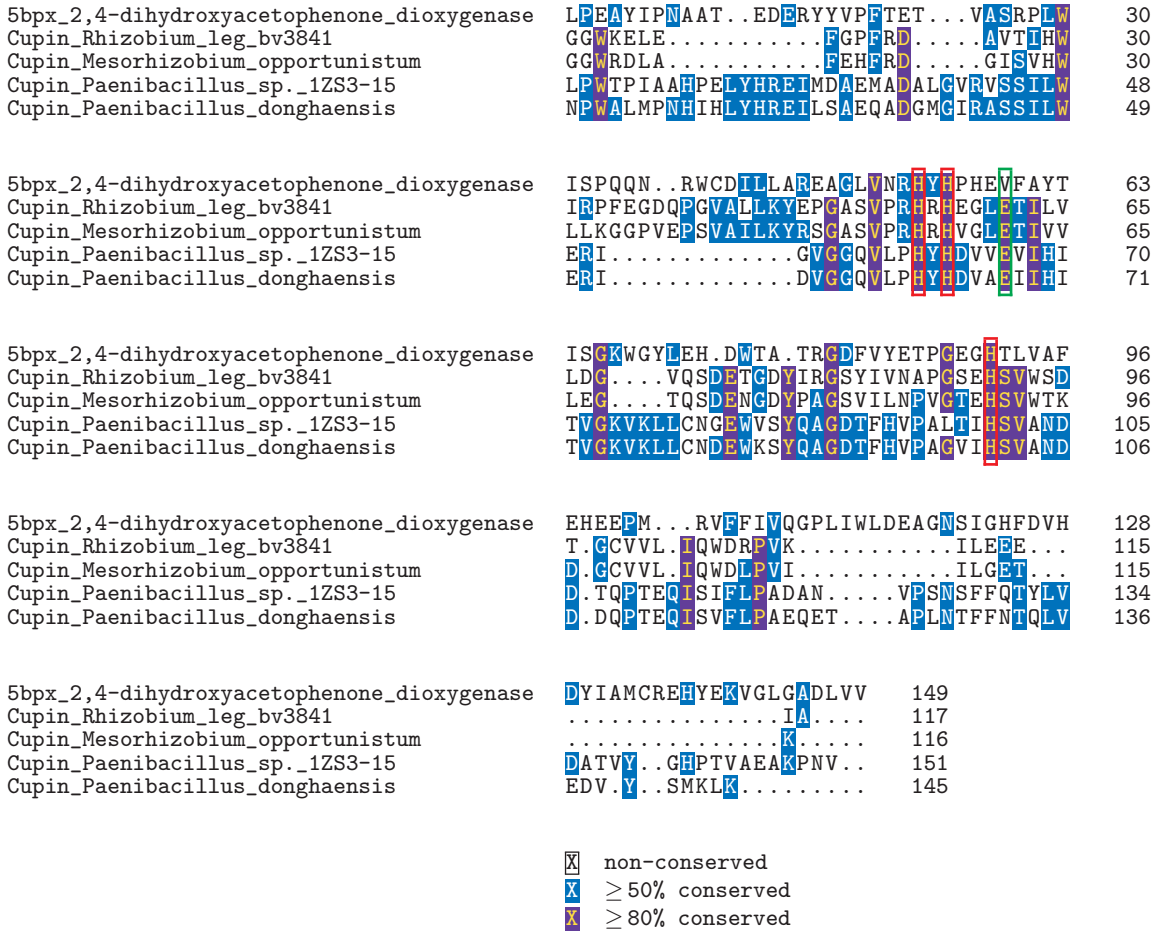

Figure 3.9: Multiple Sequence Alignment of Cupin Decarboxylase sequences with related PDB structure 5BPX:
Sequences are named by PDB ID when possible and aligned using ClustalΩ. Shading of residues indicates sequence conservation and the conserved metal binding ligand residues are highlighted in red while the glutamate residue highlighted in green is an additional ligand also found in the oxalate decarboxylase (PDB 1J58). Paenibacilli and rhizobia sequences come from different clades of cupin decarboxylases. Figure created using TexShade

These residues are three histidines and from the modelling, a potential glutamate residue which is also found in the known structure of the manganese containing oxalate decarboxylase (PDB 1J58). The *Rhizobium* Cupin sequence was selected to test for carboxybiruet decarboxylase function as the BiuH sequence from the same organism had been characterized previously[13,14]. Evidence of metal binding of Cupin was apparent as when the protein was purified it had a blue chromophore and upon adding 1,10 phenanthrolein, a divalent metal ion chelator, produced a red color complex. ICP-OES analysis revealed iron and zinc to be bound by Cupin in similar proportions but more experiments will need to be done to know which metal ion constitutes the activity. The estimated occupancy of iron and zinc in Cupin was 18 and 27%, respectively. Full occupancy was not observed, most likely due to the use of LB media for protein expression which was not supplemented with additional metals. The coupled enzyme experiment was setup for Cupin, as done for TrtB, but also adding chelator as a treatment to probe whether the metal that binds Cupin is involved in catalysis of the decarboxylation.

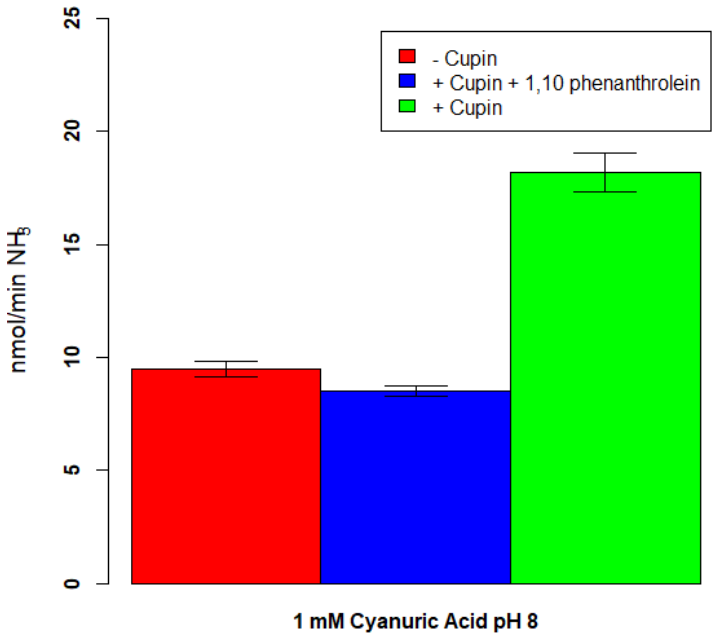

Figure 3.10: Activity of Cupin analogous to TrtB that is Metal Dependent:
The addition of Cupin can see a rate enhancement of ammonia release by increasing the steady state concentration of biuret in a coupled enzyme system of AtzD and BiuH. Chelation of the metal binding Cupin with 1,10 phenanthrolein sees the loss of the decarboxylase function. Error bars indicate one standard deviation of the mean.

As seen in Figure 3.10, the rate is enhanced when adding Cupin and chelating the metal from the cupin protein sees its activity abolished and a rate of ammonia release equal to the no Cupin sample. This indicates that Cupin is analogous to TrtB in function despite being structurally divergent. In terms of taxonomy, Cupin decarboxylase is found in alphaproteobacteria such as Rhizobia, cyanobacteria and firmicutes while the TrtB sequence is found in beta, gamma proteobacteria and actinobacteria.

3.4 Discussion

Triuret metabolism is tightly regulated in *Herbaspirillum* sp. BH-1 and the bioinformatics of TrtA suggest there is a strong selection pressure as the operons containing TrtA show

evidence for active transport and possessing the carboxybiuret decarboxylase which is a convergent evolution in different taxa.

Tight regulation of the TrtA operon in Herbaspirillum sp. BH-1

The induction of triuret metabolism is specific to biuret and triuret, and with a similar doubling time for growth on ammonium chloride, suggests active transport which is supported by the ABC transporter cassette present in the operon (Figures 3.4,3.6). While further investigation needs to be done to determine which transcription factors bind the promoter region of this operon to pinpoint the suppression mechanism there is an interesting observation of the number of ABC transporter genes that may provide insight. Typically ABC cassettes have four genes with one encoding a nucleotide binding domain (NBD) and two genes encoding transmembrane domains (TMD), the fourth gene encodes for the substrate binding domain (SBD). The ABC cassettes in TrtA operons have four genes as well but with one gene being almost twice as large as the other genes, which is not common. This large gene possesses a nucleotide binding domain at the N-terminus and at the C-terminus, a 300aa domain of unknown function. This observation is very similar to the transport of nitrate/nitrite in a cyanobacterium (*Synechocystis* sp.) where it was discovered that suppression of the nitrate assimilation in ammonium-sufficient conditions was due to inhibition of transport rather than suppressing the transcription of the operon[44]. In the study, the large ABC transporter gene was truncated to only have the NBD which removed the effector domain and as a result there was no more suppression of nitrate/nitrite transport in ammonium-sufficient conditions. This could also be the case in *Herbaspirillum* for triuret and for other nitrogenous compounds like urea or cyanuric acid that have similar ABC cassettes so as to tightly regulate the operons with potentially only one effector. In the nitrate transport example, a knockout of the nitrogen regulatory protein *glnB*, which senses α-ketoglutarate levels, also eliminated suppression by ammonia but it was inconclusive whether *glnB* interacts directly with the effector domain on the transporter[44]. If this is an acceptable theory for triuret regulation, then the transcription factor (TrtR) that is in the operon most likely binds triuret or biuret to cause induction and qPCR, gel-mobility shift assays would need to be done to find if the

transcription factor is a repressor when unbound or an enhancer when bound.

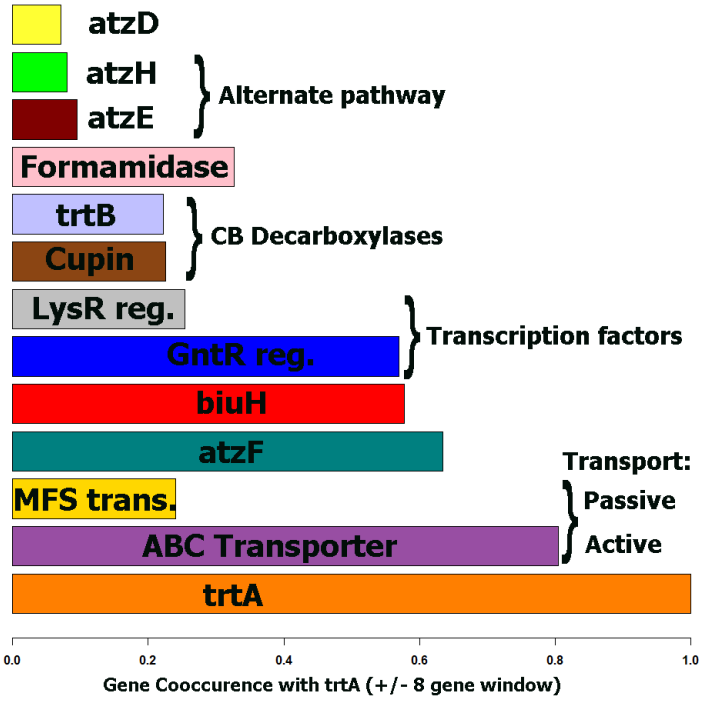

Figure 3.11: Gene Cooccurence with TrtA:
Gene contexts with a ±8 gene window around 523 bacterial TrtA sequences from RefSeq genomes were counted for the genes above. Since ABC transporters are multi component, the count was scaled down to the average number of ABC transporter genes per TrtA observed (n=4). Gene contexts were created using RODEO.

Convergent evolution of the Carboxybiuret Decarboxylase function

Around 44% of TrtA sequences from RefSeq genomes have either TrtB or a Cupin gene in the operon which are both equally prevalent (Figure 3.11). In these proportions both enzymes appear to have similar contributions to fitness and the question is now do they operate by similar mechanisms. Essentially, the decarboxylation needs a proton donor to protonate the nitrogen bonded with the carboxylate and in TrtB, the tyrosine in the active site most likely is this proton donor. Although in Cupin, the carboxylate group of carboxybiuret most likely binds to the metal ion but it is unlikely, from the homology model, that there is a residue in the active site that may serve as a proton donor. The

Cupin protein would have to be crystallized to learn more about its mechanism and the stable analog of carboxybiuret, 1-nitrobiuret, could possibly be an inhibitor of TrtB and Cupin, potentially making co-crystals. These co-crystals could then show the binding mode of carboxybiuret in the active site and elucidate the mechanism of both enzymes. The role of TrtB and Cupin does not only increase the rate of triuret mineralization but also reduces the selective pressure to have metabolism go through the AtzEG pathway, which hydrolyzes carboxybiuret to dicarboxyurea (Figure 3.1). This lower pathway has a co-occurence with TrtA at around 10% in the RefSeq database while the upper pathway through BiuH is around 60% (Figure 3.11). There are a few cases where a gene context has both pathway genes and these organisms may see a high flux of triuret and have BiuH to prevent any metabolic dead ends.

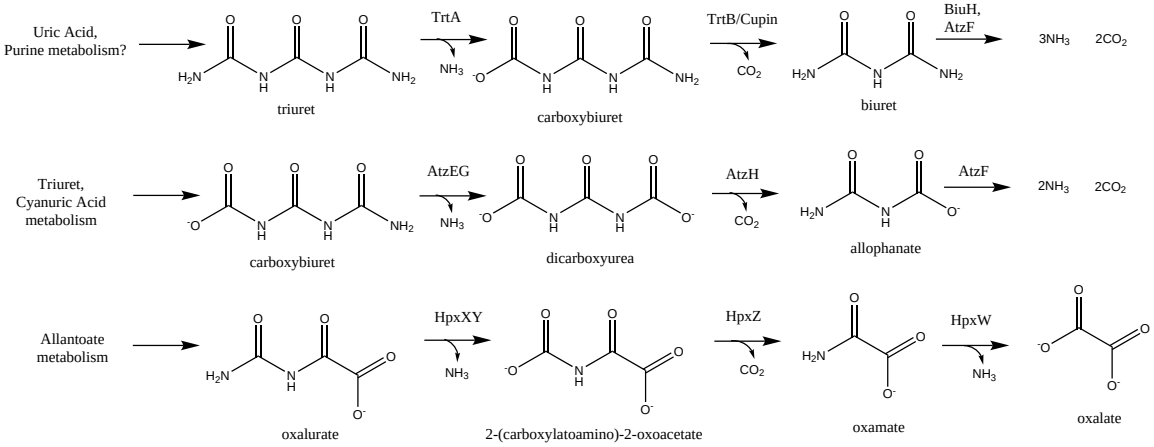

Figure 3.12: Putative function of the gene *hpxZ* in the Allantoate metabolism pathway:
Reaction schemes of metabolic pathways involving TrtB, AtzH and the homolog HpxZ from the allantoate degradation pathway. This function of HpxZ is putative and inferred by the functions of TrtB and AtzH as decarboxylases. Scheme drawn using ChemDraw.

As for TrtB, it appears that there is a distant homolog that catalyzes a similar reaction in the allantoate degradation pathway of *Klebsiella pneumoniae* by the enzyme HpxZ (Figure 3.12)[45]. There are many similarities in the pathways as the metabolites are all planar and there is homology between HpxXY, AtzEG and AtzF while TrtB, AtzH and HpxZ are also homologous to each other. As it is speculated that the source of triuret comes from uric acid metabolism, it is interesting to see a similar degradation pathway

also with uric acid as its source. In the regulation experiments with uric acid as the sole nitrogen source, there was no strong evidence that TrtA is induced in this condition, suggesting that uric acid may need an additional factor (i.e. oxidative conditions) in order to produce triuret and is more likely to be non-enzymatic (Figure 3.4. The uric acid degradation pathway is well characterized to go through allantoin and is pervasive in bacterial genomes so it remains elusive how the TrtA operon genes are useful except for artificial input of triuret during the anthropocene.

Insights of Triuret Metabolism in the Microbiome

Triuret metabolic genes interestingly come from organisms with genera synonymous with plant-associated bacteria (Figure 3.3). Nearly a third of the TrtA genes are from Rhizobial genomes (*Rhizobium*, *Bradyrhizobium*,*Agrobacterium*) which form nodules with legume plants and fix nitrogen in symbiosis. Another third, approximately, come from endophytes (beta-, gamma-proteobacteria) and actinorhizal bacteria (Frankia, Gordonia) that form nodules, different from rhizobia, with dicot plants (flowering plants). A possible connection with triuret and plants is the role uric acid metabolism as the main storage of nitrogen in plants. In plant nodules, uric acid is formed from the assimilation of nitrogen produced by bacterial endosymbionts and then is transported out through the rest of the plant as allantoin[46]. The high flux of uric acid in this environment could generate triuret as a minor product by oxidation, most likely non-enzymatically. Superoxide and nitric oxide species are present in nodules and can form peroxynitrite, a known oxidant of uric acid to produce triuret[47,48]. In most of the bacteria, triuret is transported actively or sometimes passively with a MFS-like transporter (in *Bradyrhizobium*, actinobacteria sp.), indicating that the source of triuret is coming from outside the cell and in high flux. So far the regulation of triuret metabolism has been characterized in one species and potentially, in many other organisms, the regulation could be similar. The *trtA* gene contexts show two different family types of transcriptional regulators, GntR and LysR, which in some frequency are transcribed with the TrtA operon (beta-, gamma-proteobacteria, like *Herbasprillum*) and in Rhizobia, the transcription factor is transcribed in the opposite direction. In this latter case, the regulation may be more complex with potential binding

of other transcription factors (i.e NtrC) for induction during nitrogen starvation or some other global regulation. In 30% of the gene contexts, there is a co-occuring formamidase (amiF) that by homology model appears to be a true formamidase, with ∼48% sequence identity on average to the characterized formamidase from *Heliobacter pylori* (PDB 2DYU)[49]. This enzyme produces formate, which can help generate NADH, quinol or cytochrome reducing equivalents with formate dehydrogenase. In relation to other nitrogen metabolism, formate can be a dependent cofactor for the cytochrome c nitrite reductase but it is still puzzling what the role of formamidase is in the TrtA operon[50]. Several enzymes have been discovered from the TrtA operon in this study and few unknowns remain from the genomic context but a lot remains to be seen about the role of triuret metabolism in nature. If the plant association is credible then it would be interesting to see what phenotypic changes a *trtA* gene knockout would cause to nodulation and plant growth. Not all nodulating bacteria have the TrtA operon but then some rhizobia prefer to nodulate with certain plants so the difference may lie there. Large triuret granules have been observed in freshwater amoebas (*Amoeba proteus*) and it would not be surprising if bacterial symbionts in amoebae mineralize triuret[10].

Chapter 4

Application and Future Research

4.1 Triuret: A potential N fertilizer

The mysterious role of triuret metabolism is already very intriguing but what is also exciting is the prospect of triuret being a nitrogen fertilizer in agriculture. Given that triuret is much less soluble than urea and other nitrogen fertilizers, there is a great opportunity to demonstrate that a better alternative for agriculture, is triuret. The enzymes in the triuret degradation pathway have been characterized, which can release all of the nitrogen as ammonia and the regulation of the metabolism can shut off in nitrogen sufficient conditions to slow the release even more (Chapters 2,3). The triuret hydrolase gene is rare in recorded genomes (<1%) and compared to urease, which is in ∼35% of RefSeq bacterial genomes, the activity in the soil is then several orders of magnitude higher for urea than triuret. The low aqueous solubility of triuret also allows for the particle size to strongly affect the dissolution rate and thereby control the release of N fertilizer[51]. Typical application of urea fertilizer is in granules or prills with size of 1.5-2.5mm diameter to limit dissolution but also for practical application, as a fine powder can be taken up by the air quite easily. This formulation dissolves in the soil within two weeks and according to Hays et al, a particle size for triuret around 1.4mm is only 30% nitrified (to NO_3^-) in six weeks[51]. This rate of release is similar to the N uptake of corn, which is maximal at 9 weeks, and triuret has therefore a better shot than urea to deliver

nitrogen efficiently and minimize the losses that happen through volatilization and leaching. Currently, only 30% of urea nitrogen applied is taken up by crops while there are hopes that triuret can be at least 60% efficient as a nitrogen fertilizer.

4.2 Industrial synthesis

One barrier to commercialization of triuret as a fertilizer is the inexpensive industrial production that is needed to be cheaper than urea fertilizer. The best process to date with a 70% yield is a reaction of urea and hydrogen chloride to make mainly triuret and ammonium chloride [3]. This crude product could potentially be a fertilizer on its own with fast and slow release sources of nitrogen combined but will likely be more expensive than urea, although, cheaper than other slow release fertilizers that are more than twice the price of urea. A new process would have to be invented to compete with the price of urea and which is theorized in the figure below.

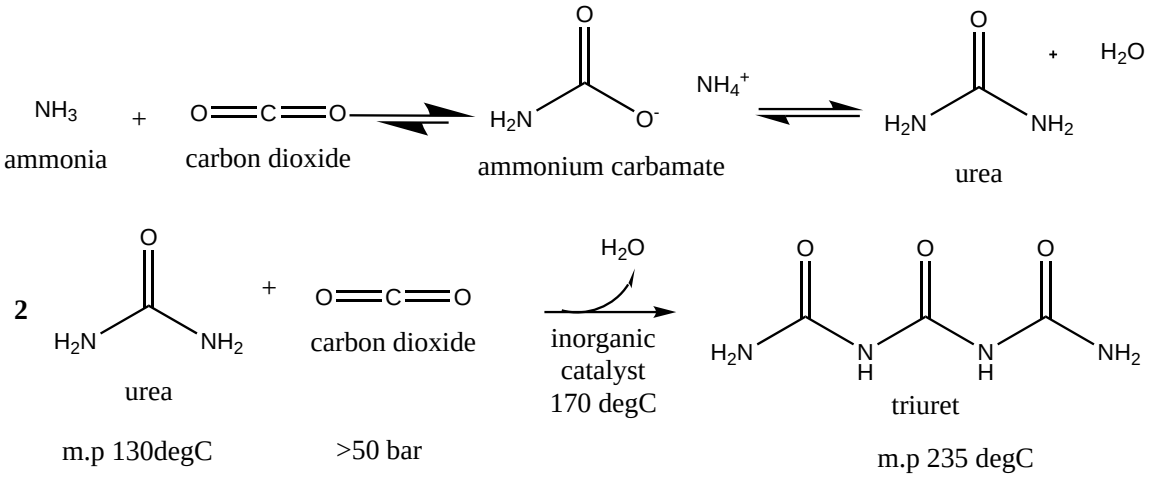

Figure 4.1: Proposed Industrial synthesis for Triuret
Coupling the first two steps of the current urea industrial process a catalyst could potentially produce triuret from a condensation reaction of urea and CO_2. The formation of ammonium carbamate is very fast but the condensation is slow and requires a sophisticated, continuous process for large production. Coupling the urea process to a triuret synthesis process would potentially speed up the reaction by driving the equilibrium forward.

The new process would work in similar conditions as the current urea process, working in high pressure CO_2 and NH_3 at an elevated temperature. The current process is relatively

slow and needs to be sophisticated as there is a fast step to form ammonium carbamate but is followed by a very slow condensation to urea. This is because the reaction temperatures are above the melting point of urea and an equilibrium still exists, with the intermediates in the liquid phase, which then requires the process to be continuous[52]. Hypothetically, two ureas could condense with one CO_2 to produce triuret but it would require a catalyst to lower the energy barrier. Triuret would then precipitate at the same reaction temperature due to its high melting point and drive the equilibrium forward, reducing production time and costs. The catalyst would most likely be an inorganic catalyst, that contains a transition metal with complex ligands coordinating it. There are several examples of ureas being made by such catalysts from CO_2 and amines and these could be good starting points to catalyze triuret formation[53,54,55]. If this can be achieved then triuret production could be significantly cheaper and require less sophisticated equipment to do so.

4.3 Fertilizer Demonstration

There are no reports on triuret used as a fertilizer and there will need to be agricultural demonstrations to sway farmers to adopt this new practice. In addition, the efficacy of using triuret is still not known and this will require ^{15}N studies to see if % incorporation in crops is significantly higher than using urea. A metabolite of triuret degradation, biuret, has been reported to be toxic to plants as it is an impurity in urea fertilizer. Biuret, unlike triuret, is a known chelator of copper and possibly other divalent metal ions and this may cause metal deficiencies in the crops but also may inhibit bacterial processes such as nitrification and nitrogen fixation, also critical for plants[2,56]. This will need to be looked into for triuret and the formulation of triuret must address these effects should they occur.

4.4 Conclusion and Future Research

Industrially produced nitrogen fertilizers is only a century old phenomenon and there should not be resignation to the agricultural practices that are in place now as there is

potential to change. Prior to the use of these fertilizers, bat and sea-bird guano was highly sought as a fertilizer as it contained ideal amounts of nitrogen, phosphorus and potash (potassium)[57]. The nitrogen in the guano, mostly in the form of uric acid, has similar solubility as triuret and can be considered the "ultimate fertilizer", given that it is a nitrogen waste product in manures and has been amending soils with nitrogen for millennia. The problem is uric acid cannot be made inexpensively on an industrial scale but the closest molecule to it, that can be produced industrially, is triuret. Both compounds have the same moles of nitrogen and both may be connected metabolically. The discovery of the triuret hydrolase and therefore, triuret metabolism, also strengthens the claims of uric acid being a great antioxidant[8]. Uric acid can scavenge chemical oxidants which can lead to triuret formation but also can absorb UV-light and be photo-oxidized to generate other oxidation productions including a potential precursor of cyanuric acid, oxanate[58].

Moving forward I will pursue engineering the triuret hydrolase (TrtA) to become a biuret hydrolase (BiuH) and develop a rational explanation as to how this evolution occurred to discriminate biuret and triuret with near identical active site residues. In addition, TrtA and BiuH have potential, with a single amino acid substitution, to hydrolyze guanidine derivatives of triuret and biuret, guanylbiuret and guanylurea, which the latter is a emerging pollutant from the use of the obesity and type-II diabetes drug, metformin[59]. The engineering of TrtA could help create a catalyst for the remediation of guanylurea and potentially other compounds.

In regards to the regulation of triuret metabolism in *Herbaspirillum* sp. BH-1, the ammonium suppression mechanism will be investigated with the hypothesis that the active transport is inhibited by a nitrogen regulatory protein, similar to the regulation of nitrate/nitrite assimiliation in the cyanobacterium, *Synechocystis* sp. Strain PCC 6803[44]. If this is the case, it would be the first example in proteobacteria and likely infer the suppression mechanism of other nitrogen metabolites that have the same 4-gene ABC cassettes (i.e urea, cyanuric acid, etc.).

In addition to the science, I will work towards developing triuret into a nitrogen fertilizer;

Collaborating with Dr. Rosen in Soil Science to find the appropriate formulation of triuret for various crops. Fertilizer practice is a worldwide phenomenon and a change to a more efficient alternative, like triuret, could make a monumental impact and just like how the whole world began to use these simple fertilizers some 100 years ago, the world can make a simple change again to lead us into the next paradigm of agroecological management and in solving other environmental problems.

Bibliography

[1] H. Scherer, K. Mengel, G. Kluge, and K. Severin. Fertilizers, 1. General. *Ullmann's Encyclopedia of Industrial Chemistry*, 14:171–197, 2009.

[2] R.C. Haworth and F.G. Mann. Some Properties of Urea, Biuret, and Triuret. *Journal of the Chemical Society*, pages 603–606, 1943.

[3] Scholven Chemie Aktiengesellschaft. Improvements in or relating to the Production of Triuret. Patent no. GB1156028A, June 25 1969.

[4] S.M. Cameron. *Biuret Hydrolase and Cyanurc Acid Hydrolase: Enzymes for Metabolism and Detection of s-triazines.* PhD thesis, University of Minnesota, St. Paul, MN, 8 2013.

[5] S.M. Cameron, K. Durchschein, J.E. Richman, M.J. Sadowsky, and L.P. Wackett. A New Family of Biuret Hydrolases Involved in S-Triazine Ring Metabolism. *ACS Catalysis*, 1:1075–1082, 2011.

[6] D. Carlstrom and H. Ringertz. The Molecular and Crystal Structure of Triuret . *Acta Crystallographica*, 18:307–313, 1965.

[7] J. Bremner and M. Krogmeier. Reactions of peroxynitrite with uric acid: Formation of reactive intermediates, alkylated products and triuret, and in vivo production of triuret under conditions of oxidative stress. *Nucleosides Nucleotides Nucleic Acids*, 28:118–149, 2009.

[8] D. Hooper, S. Spitsin, J. Champion, G. Dickson, I. Chaudhry, and H. Koprowski. Uric acid, a natural scavenger of peroxynitrite, in experimental allergic encephalomyelitis and multiple sclerosis. *PNAS*, 95:675–680, 1998.

[9] K.M. Kim, G.N. Henderson, R.F. Frye, C.D. Galloway, N. Brown, M.S. Segal, W. Imararam, A. Angerhofer, and R.J. Johnson. Simultaneous determination of uric acid metabolites allantoin, 6-aminouracil, and triuret in human urine using liquid

chromatography–mass spectrometry. *J Chromatogr B Analyt Technol Biomed Life Sci.*, 877:65–70, 2009.

[10] J. Griffin. Identification of Ameba Crystals II. Triuret in Two Crystal Forms. *Biochim. Biophys. Acta*, 47:433–439, 1961.

[11] J. Engelhardt, J. Friis, and K.M. Moller. Investigations of a Triuret Decomposing Enzyme in *Corynebacterium Michaganense*. *Comptes Rendus Des Travaux Du Laboratoire Carlsberg*, 40(20):360–396, 1976.

[12] P.M. Gilbert, J. Harrison, C. Heil, and S. Seitzinger. Escalating worldwide use of urea – a global change contributing to coastal eutrophication. *Biogeochemistry*, 77: 441–463, 2006.

[13] S.L. Robinson, J.P. Badalamenti, A.G. Dodge, L.J. Tassoulas, and L.P. Wackett. Microbial biodegradation of biuret: defining biuret hydrolases within the isochorismatase superfamily. *Applied and Environmental Microbiology*, 20:2099–2111, 2018.

[14] L. Esquirol, T.S. Peat, M. Wilding, D. Lucent, N.G. French, C.J. Hartley, J. Newman, and C. Scott. Structural and biochemical characterization of the biuret hydrolase (BiuH) from the cyanuric acid catabolism pathway of *Rhizobium leguminasorum bv. viciae* 3841. *PLOS One*, 13:1–20, 2018.

[15] C.S Veneable. The Action of Hydrogen Peroxide Upon Uric Acid. *JACS*, 40: 1099–1120, 1918.

[16] W. Kabsch. XDS. *Acta Cryst. D*, 66:125–132, 2010.

[17] M.D. Winn et al. Overview of the CCP4 suite and current developments. *Acta Cryst. D*, 67:235–242, 2011.

[18] P. Emsley, B. Lohkamp, W. Scott, and K. Cowtan. Features and Development of Coot. *Acta Cryst. D*, 66:486–501, 2010.

[19] T.P. Murray, E.R. Austin, and R.G. Howard. Synthesis of ^{15}N-Labelled Urea and Methylenediurea. *Journal of Labelled Compounds and Radiopharmaceuticals*, 22(12): 1251–1259, 1985.

[20] Y. Ogata, A. Kawasaki, and N. Okumura. Kinetics of the Condensation of Urea with Acetaldehyde. *Journal of Organic Chemistry*, 30(5):1636–1639, 1964.

[21] A.M. Goral, K.L. Tkaczuk, M. Chruszcz, O. Kagan, A. Savchenko, and Minor W. Crystal structure of a putative isochorismatase hydrolase from *Oleispira antarctica*. *J Struct Funct Genomics*, 13:27–36, 2012.

[22] A. Bar-Even, E. Noor, Y. Savir, W. Liebermeister, D. Davidi, D.S. Tawfik, and R. Milo. The Moderately Efficient Enzyme: Evolutionary and Physicochemical Trends Shaping Enzyme Parameters. *Biochemistry*, 50:4402–4410, 2011.

[23] L. Esquirol, T.S. Peat, M. Wilding, Jian-Wei Liu, N.G. French, C.J. Hartley, H. Onagi, T. Nebl, C.J. Easton, J. Newman, and C. Scott. An unexpected vestigial protein complex reveals the evolutionary origins of an s-triazine catabolic enzyme. *J Biol Chem*, 2018.

[24] N. Shapir, M.J. Sadowsky, and L.P. Wackett. Purification and Characterization of Allophanate Hydrolase (AtzF) from *Pseudomonas* sp. Strain ADP. *Journal of Bacteriology*, 187(11):3731–3738, 2005.

[25] J.L. Seffernick, J.S. Erickson, S.M. Cameron, S. Cho, A.G. Dodge, J.E. Richman, M.J. Sadowsky, and L.P. Wackett. Defining Sequence Space and Reaction Products within the Cyanuric Acid Hydrolase (AtzD)/Barbiturase Protein Family. *J. Bacteriol.*, 194:4579–4588, 2012.

[26] M. Lardi, Aguilar C., A. Pedrioli, U. Omasits, A. Suppiger, N. Carcamo-Oyarce, Schmid, C.H. Ahrens, L. Eberl, and G. Pessi. σ^{54}-Dependent Response to Nitrogen Limitation and Virulence in *Burkholderia cenocepacia* Strain H111. *Appl Env Microbiol*, 81:4077–4089, 2015.

[27] L. Noindorf, A.C. Bonatto, R.A. Monteiro, E.M. Souza, L.U. Rigo, F.O. Pedrosa, M.B. Steffens, and L.S. Chubatsu. Role of PII proteins in nitrogen fixation control of Herbaspirillum seropedicae strain SmR1. *BMC Microbiol*, 11, 2011.

[28] E.M. Souza, F.O. Pedrosa, M. Drummond, L.U. Rigo, and M.G. Yates. Control of Herbaspirillum seropedicae NifA Activity by Ammonium Ions and Oxygen. *J Bacteriol*, 181:681–684, 1999.

[29] M.T. Emori, L.F. Tomazini, F.O. Pedrosa, L.S Chubatsu, and Oliveira M. The deuridylylation activity of Herbaspirillum seropedicae GlnD protein is regulated by the glutamine:2-oxoglutarate ratio. *Biochim Biophys Acta Proteins Proteom*, 1866: 1216–1223, 2018.

[30] F. Rego, F.O. Pedrosa, L.S. Chubatsu, G. Yates, R. Wassem, M. Steffens, L. Rigo, and E.M. Souza. The expression of *nifB* gene from *Herbaspirillum seropedicae* is dependent upon the NifA and RpoN proteins. *Can J. Microbiol*, 52:1199–1207, 2006.

[31] I. Suvorova, Y. Korostelev, and M. Gelfand. GntR Family of Bacterial Transcription Factors and Their DNA Binding Motifs: Structure, Positioning and Co-Evolution. *PloS ONE*, 10, 2015.

[32] M. Zheng, D.R. Cooper, N.E Grossoehme, M. Yu, L.W. Hung, M. Cieslik, and et al. Structure of Thermotoga maritima TM0439: implications for the mechanism of bacterial GntR transcription regulators with Zn^{2+} binding FCD domains. *Acta Crystallogr D Biol Crystallogr*, 65:356–365, 2009.

[33] J.A Gerlt, J.T. Bouvier, D.B. Davidson, H.J. Imker, Sadkhin B., D.R. Slater, and K.L Whalen. Enzyme Function Initiative-Enzyme Similarity Tool (EFI-EST): A web tool for generating protein sequence similarity networks. *Biochimica et Biophysica Acta - Proteins and Proteomics*, 1854:1019–1037, 2015.

[34] P. Shannon, A. Markiel, O. Ozier, N.S. Baliga, J.T. Wang, D. Ramage, N. Amin, B. Schwikowski, and T. Ideker. Cytoscape: a software environment for integrated models of biomolecular interaction networks. *Genome Research*, 13:2498–2504, 2003.

[35] S.R. Eddy. Accelerated profile HMM searches. *PLoS Comput Biol*, 7, 2011.

[36] J.I. Tietz, C.J. Schwalen, P.S. Patel, T. Maxson, P.M. Blair, and *et al.* Tai, H.C. A new genome-mining tool redefines the lasso peptide biosynthetic landscape. *Nat Chem Biol*, 13, 2017.

[37] A. Stamatakis. RAxML version 8: a tool for phylogenetic analysis and post-analysis of large phylogenies. *Bioinformatics*, 30:1312–1313, 2014.

[38] R.E. Parales, J.E. Adamus, N. White, and H.D. May. Degradation of 1,4-dioxane by an actinomycete in pure culture. *Appl Environ Microbiol*, 60:4527–4530, 1994.

[39] Q. Li, J.L Seffernick, M.J. Sadowsky, and L.P. Wackett. Thermostable Cyanuric Acid Hydrolase from *Moorella thermoacetica* ATCC 39073. *Appl Environ Microbiol*, 75: 6986–6991, 2009.

[40] V. Garcia-Gonzalez, F. Govantes, O. Porrua, and E. Santero. Regulation of the Pseudomonas sp. Strain ADP Cyanuric Acid Degradation Operon. *Journal of Bacteriology*, 187:155–167, 2005.

[41] L. Esquirol, T.S. Peat, M. Wilding, C.J. Hartley, J. Newman, and C. Scott. A novel decarboxylating amidohydrolase involved in avoiding metabolic dead ends during cyanuric acid catabolism in Pseudomonas sp. strain ADP. *PLoS ONE*, 13, 2018.

[42] J.M Dunwell, A. Purvis, and S. Khuri. Cupins: the most functionally diverse protein superfamily? *Phytochemistry*, 65:7–17, 2004.

[43] J. Guo, P. Erskine, A.R. Coker, J. Gor, S.J. Perkins, S.P. Wood, and J.B. Cooper. Extension of resolution and oligomerization-state studies of 2,4'-dihydroxyacetophenone dioxygenase from Alcaligenes sp. 4HAP. *Acta Crystallogr. Sect.F*, 71:1258–1263, 2015.

[44] M. Kobayashi, N. Takatani, M. Tanigawa, and T. Omata. Posttranslational Regulation of Nitrate Assimilation in the Cyanobacterium *Synechocystis* sp. Strain PCC 6803. *J Bacteriol*, 187:498–506, 2005.

[45] K Guzman, E. Campos, L. Aguilera, L. Toloza, R. Gimenez, J. Aguilar, L. Baldoma, and J. Badia. Characterization of the gene cluster involved in allantoate catabolism and its transcriptional regulation by the RpiR-type repressor HpxU in *Klebsiella pneumoniae*. *International Microbiology*, 16:165–176, 2013.

[46] H.C. Pelissier, Frerich A., M. Desimone, K. Schumacher, and Tegeder M. PvUPS1, an Allantoin Transporter in Nodulated Roots of French Bean. *Plant Physiology*, 134: 664–675, 2004.

[47] K.M. Robinson, J.T. Morre, and J.S. Beckman. Triuret: a novel product of peroxynitrite-mediated oxidation of urate. *Archives of Biochemistry and Biophysics*, 423:213–217, 2004.

[48] C. Lindermayr and J. Durner. Interplay of Reactive Oxygen Species and Nitric Oxide: Nitric Oxide Coordinates Reactive Oxygen Species Homeostasis. *Plant Physiology*, 167:1209–1210, 2015.

[49] C. Hung, J. Liu, W. Ciu, S. Huang, Hwang J., and W. Wang. Crystal Structure of Helicobacter pylori Formamidase AmiF Reveals a Cysteine-Glutamate-Lysine Catalytic Triad. *J Biol Chem*, 282:12220–12229, 2007.

[50] O. Einsle. Structure and function of formate-dependent cytochrome c nitrite reductase, NrfA. *Methods in Enzymology*, 496:399–422, 2011.

[51] J.T. Hays and W.B. Hewson. Controlled Release Fertilizers by Chemical Modification of Urea: Triuret. *Journal of Agricultural and Food Chemistry*, 21(23):498–499, 1973.

[52] S. Lemkowitz, J. Zuidam, and P. van den Berg. Phase Behaviour in the Ammonia-Carbon Dioxide System at and above Urea Synthesis Conditions. *J Appl Chem Biotechnol*, 22:727–737, 1972.

[53] Y. Li, X. Fang, K. Junge, and M. Beller. A General Catalytic Methylation of Amines Using Carbon Dioxide. *Angewandte Chemie*, 52:9568–9571, 2013.

[54] K. Beydoun, T. vom Stein, J. Klankermayer, and W. Leitner. Ruthenium-Catalyzed Direct Methylation of Primary and Secondary Aromatic Amines Using Carbon Dioxide and Molecular Hydrogen. *Angewandte Chemie*, 52:9554–9557, 2013.

[55] Q. Liu, L. Wu, R. Jackstell, and M. Beller. Using carbon dioxide as a building block in organic synthesis. *Nature Communications*, 6, 2014.

[56] K. Sahrawat. Effect Of Biuret Content On Transformation Of Urea Nitrogen Soil. *Soil Biol Biochem*, 9:173–175, 1977.

[57] P. Szpak, F. Longstaffe, J. Millaire, and C. White. Stable Isotope Biogeochemistry of Seabird Guano Fertilization: Results from Growth Chamber Studies with Maize (*Zea Mays*). *PLoS ONE*, 7, 2012.

[58] B. Hojerup and K.M. Moller. Triuret: A Survey of the Literature. *Comptes Rendus Des Travaux Du Laboratoire Carlsberg*, 39(8):168–289, 1973.

[59] J. Straub, D. Caldwell, T. Davidson, V. D'Aco, K. Kappler, P. Robinson, B. Simon-Hettich, and J. Tell. Environmental risk assessment of metformin and its transformation product guanylurea. I. Environmental fate. *Chemosphere*, 216: 844–854, 2019.

Appendix A

Supplementary Information

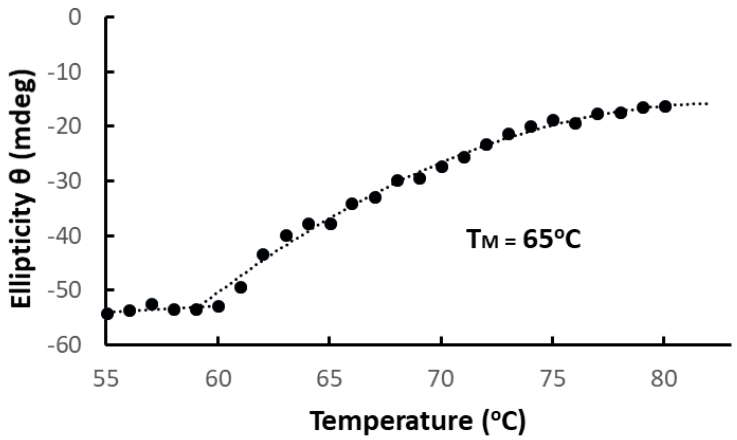

Figure A.1: Thermal Stability of TrtA
Melting temperature of TrtA with cleaved His-tag was determined by Circular Dichroism and calculated to be $\sim 65^{o}$C. Ellipticity was measured at wavelength 220nm with a 1^{o}C/min temperature gradient from $45-80^{o}$C.

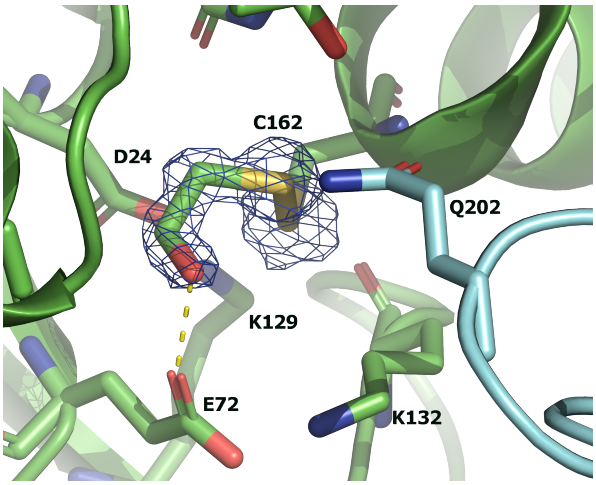

Figure A.2: TrtA Active Site with BME Adduct on Catalytic Cysteine
2Fo-Fc map for the BME adduct on C162 of TrtA WT contoured at 1σ. Residue color indicates which chain the residue is from. Polar contacts made with BME are marked by yellow dash.